Protocol to Determine the Optimal Placement of Riparian/Buffer Strips in Watersheds

Start Date: 03/01/2005

End Date: 05/31/2006

Congressional District: 2nd and 3rd Oklahoma Congressional Districts

Focus Category: COV, HYDROL, M&P, MET, MOD, NPP, NU, SED, SW, WQL

Descriptors: Targeting, Riparian, SWAT, REMM, Spavinaw, GIS, Flow Accumulation, Phosphorus, Sediment, Buffer, Model

Principal Investigators: Daniel E. Storm[1], Michael J. White[1], Glenn O. Brown[1], Michael D. Smolen[1], and Ranbir S. Kang[2]

[1]Department of Biosystems and Agricultural Engineering, Division of Agricultural Sciences and Natural Resources, Oklahoma State University. [2]Department of Geography, College of Arts and Sciences, Oklahoma State University.

Publications: None Pending

Table of Contents

(1) Problem and Research Objectives

(1.1) Introduction

Riparian buffers are a commonly recommended Best Management Practice (BMP) in Okalahoma and in other parts of the United States. Their use is promoted by federal programs such as the Conservation Reserve Program (CRP), Conservation Reserve Enhancement Program (CREP), Environmental Quality Incentives Program (EQIP), and various cost-share programs funded by USEPA 319(h) and state funds. Buffers are among the primary BMPs recommended by environmental agencies to reduce nonpoint sources pollution (Fields, 1992). Effectiveness of buffers in the removal of sediment and nutrients at a field scale has been extensively explored (Barling and Moose, 1994; Hill, 1996; Fennessy and Cronk, 1997; Lowrance *et al.*, 2002). However, the effect of riparian buffers placement within a watershed has not been well studied. Placement is, nevertheless, likely to have a significant effect on the effectiveness of the BMP. Optimizing overall BMP performance through proper placement is a critical issue (Tomer *et al.*, 2003; Marcelo and Conrad, 2003). Establishment of buffers is expensive and funding is limited; only a small fraction of streams within a watershed generally receive the BMP. By evaluating the effectiveness of riparian buffers at all potential sites within a watershed we can optimally place the buffers in targeted areas to generate the most environmental benefit per dollar spent.

(1.2) Objectives

The primary objective of this project was to develop a methodology to identify the optimal placement of riparian buffer strips in a watershed and to test that method in the Spavinaw Creek watershed in northeast Oklahoma. A secondary objective was to evaluate the use of SWAT and REMM models for the purpose of optimizing riparian BMP placement and to evaluate the effect of riparian buffer widths.

Since the proposal was submitted, we discovered that the secondary objective has been addressed by other research. Work elsewhere linking SWAT and REMM has progressed and it is clear that REMM and SWAT can be linked and will be useful for predicting the effects of riparian BMPs (Cerucci 2002, Amanjot 2003). It was not within the scope of this project to develop a comprehensive linkage between SWAT and REMM, since that work is currently underway by other researchers. Models such as SWAT and REMM are complex; to properly link these models in a useful manor requires a great deal of experience with both models. The linkage will certainly require involvement of the developers of both models, and is beyond both the budget and the duration of this project. For these reasons we have chosen to focus on the development of a methodology to target riparian areas based on currently available tools, and to demonstrate this methodology in the Spavinaw Creek watershed.

(1.3) Previous Work

Even though the effect of buffer placement has not been well studied, it is generally agreed that targeting areas for buffer establishment does improve the total environmental benefit. Several studies have performed targeting to identify areas for riparian buffer establishment (Table 1.1.3). The optimal placement of riparian buffers within a watershed has been based on a number of metrics, models, and or other criteria.

The primary criterion used in previous studies is landcover within the riparian corridor (Wilkinson *et al.,* 2004; Christianson *et al.*, 2005; Zhaoning *et al.*, 2005). Landcover data are readily available or can be developed from remotely sensed imagery, and can be used to asses the status of vegetation within the riparian corridor. Areas with little vegetation or erosive land uses are natural candidates for riparian BMPs.

Hydrologic models have been used by researchers to identify areas with the most potential for improvement (Wanhong and Weersink 2004; Marcelo and Conrad, 2003). In these studies two separate types of models were used to predict BMP benefits, an upland model like the Soil and Water Assessment Tool (SWAT), Erosion Productivity Impact Calculator (EPIC), or AGricultural Non-Point Source (AGNPS), and a riparian zone model such as Riparian Ecosystem Management Model (REMM). The data and computational requirements of these models are tremendous. Researchers have reduced these requirements by limiting spatial detail (resolution) and or spatial extent (area) considered, giving rise to very detailed field scale models and less detailed basin scale models.

Because basin scale models have large spatial extents, many field scale processes are aggregated or not considered. Models such as SWAT cleverly reduce the number of calculations by aggregating input GIS data into subbasins and Hydrologic Response Units (HRU). Both Wanhong and Weersink (2004) and Marcelo and Conrad (2003) used basin scale upland models (AnnAGNPS, SWAT) in conjunction with field scale riparian models (REMM, Vegetated Filter Strip (VFS)). This combination allowed both researchers to estimate pollutant reduction with riparian BMPs. SWAT and AnnAGNPS operate by aggregating individual gridcells from the original landcover, soils and elevation data into subbasins. Targeting is also aggregated to the subbasin level; a limitation of all commonly used basin scale hydrologic and nutrient models. In reality there may be optimal locations within each subbasin. This limitation is reduced by using smaller subbasins, Wanhong and Weersink (2004) and Marcelo and Conrad (2003) had average subbasin sizes of 0.51 km^2 and 1.2 km^2, respectively. To utilize the same subbasin areas for targeting riparian areas in the Lake Eucha basin or the Illinois River basin, two of Oklahoma's priority basins, would require 1,300 and 5,500 subbasins, which is excessive and beyond the limits for most models. With the current generation of models it will be problematic to resolve

both the fine scale at which riparian buffer processes operate and the spatial extent required to perform targeting in large basins.

Tomer *et al.* (2003) used terrain analysis to identify optimal locations for wetlands. They found that 57% of riparian gridcells received runoff from less than 1 acre, making these locations poor choices for riparian BMPs. A riparian area can only filter water which moves through it from adjacent areas. Therefore, when the drainage area of BMP is less than its design capacity, the less effective the practice is to the overall water quality of the basin.

(1.4) Study Area

The area selected for this study was Brush Creek and lower Beaty Creek in northeast Oklahoma, which are portions of the Lake Eucha Basin. The Lake Eucha Basin has been studied extensively by Oklahoma State University, the City of Tulsa, and the Oklahoma Conservation Commission. Data, such as IKONOS imagery, were available in the Lake Eucha Basin and not available elsewhere. These sites were selected because they contained both forested and degraded riparian areas and a variety of landcovers. The study area covered 47,000 acres within the Oklahoma portion of the Lake Eucha Basin (Figure 1.4).

Table 1.3.1 Criteria used for riparian targeting in previous studies.

Study (Reference)	Targeting Criteria
Murrumbidgee Catchment (Wilkinson *et al.*, 2004)	Remotely sensed canopy cover, estimated stream power, and SedNet predicted gulley erosion.
Turkey Creek (Christianson *et al.*, 2005)	Remotely sensed landcover weighted by unit/area estimated erosion.
Rapidan River (Tipett *et al.*, 2001)	Extensive field survey, summarized and ranked in a GIS.
Canagagigue Creek (Wanhong and Weersink, 2004)	Annualized Agricultural Nonpoint Source Pollution (AnnAGNPS) and Vegetation Filter Strip (VFS) model predicted sediment delivery.
Tipton Creek (Tomer *et al.,* 2003)	Wetness and erosion indices based on contributing area and slope.
Beijing GuanTing Watershed (Zhaoning *et al.*, 2005)	Remotely sensed landcover and stream proximity.
Townbrook Watershed (Marcelo and Conrad, 2003)	SWAT upland model and REMM riparian model Subbasin Level.

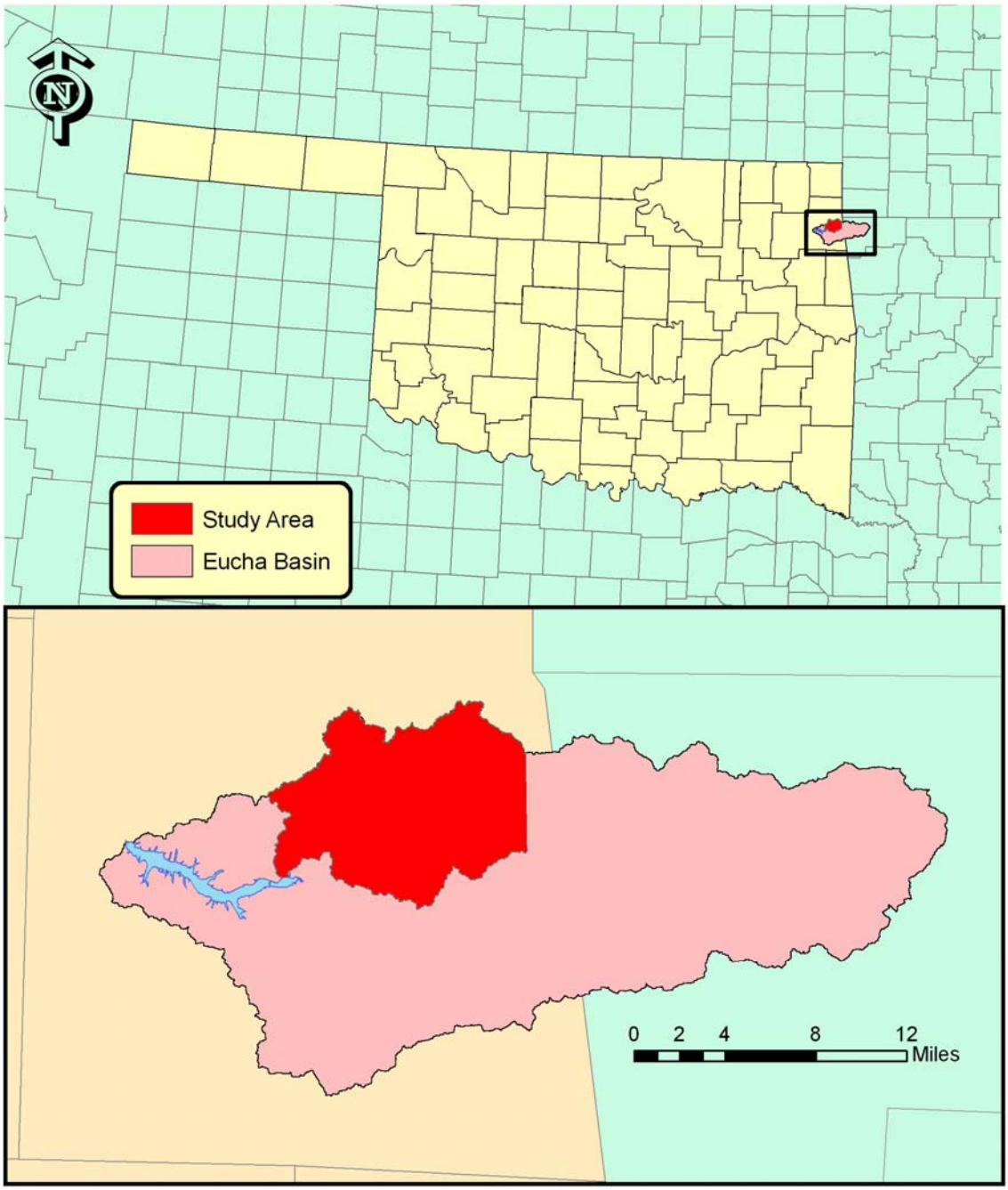

Figure 1.4 Brush Creek and lower Beaty Creek study site within the Lake Eucha Basin.

(2) Methodology

For this project, the use of models to optimally locate riparian BMPs was rejected in favor of using simpler GIS based means. Currently available watershed models, such as SWAT, must be linked with a riparian model to evaluate riparian BMPs, a significant undertaking. This linkage is currently underway by other researches and will likely become available in a few years. While models can quantitatively predict improvement by the establishment of a BMP in any location, current models lack the ability to do so with high resolution and large extents. For these reasons we believe that the best solution, given current technology, is to use simpler methods to target riparian BMPs using primarily qualitative means.

Our approach is to use multiple indicators of riparian BMP suitability and effectiveness obtainable from various GIS data and weight them into a single indicator. This master indicator will then be used to rank all possible riparian BMP sites from most to least effective. GIS derived indicators are listed below and explained in more detail in the following sections.

1) Landcover within the riparian zone
2) RUSLE gridcell predicted erosion
3) Extrapolated SWAT runoff volume and soluble phosphorus yield
4) Flow accumulation from adjacent areas
5) Stream curvature
6) Stream order and gradient

(2.1) RUSLE gridcell predicted erosion

Erosion is highly correlated with the transport of sediment-bound nutrients, including phosphorus. The Universal Soil Loss Equation (USLE) (Wischmeier and Smith, 1978) and the more recent Revised Universal Soil Loss Equation (RUSLE) (Renard *et al.*, 1991) can be applied to readily available GIS data to generate rainfall erosion estimates for large areas. USLE and RUSLE are designed to predict long term average annual soil loss using an extensive database of parameter values developed across the US. Both the USLE and RUSLE are calculated as:

$$A = R\ K\ L\ S\ C\ P$$

where R is the rainfall factor, K is the soil erodibility factor, L is the slope length factor, S is the slope gradient factor, C is the crop management factor and P is the conservation practice factor. RUSLE improves prediction over the USLE by incorporating sub factors to better represent field conditions and management.

C Factor

USLE C factors are based directly on landcover and land use. Landcover/land use is the most important contributor to erosion. The landcover data affects the amount and distribution of pasture, small grains, row crop, and forest in the basin. These landcovers are very different. Forested areas contribute little to the sediment loading, while pastures, small grains and row crops are thought to be the primary source of sediment and nutrients.

It is important that landcover data be based on the most current data available, since landcover changes over time. Therefore, landcover was derived from four meter IKONOS imagery, digital aerial photos, ground truth data points provided by the Oklahoma Conservation Commission, and a stream corridor manually digitized from IKONOS 1 meter panchromatic imagery by Oklahoma State University (OSU) personnel (Storm *et al.*, 2005). Ten IKONOS images captured February 17, 2005 were obtained and classified by Applied Analysis Inc. (AAI). An unsupervised iterative self-organizing data analysis (ISODATA) clustering algorithm was applied by AAI to define spectral categories. After several iterations these categories combined into individual landcovers (Figure 2.1.1). OSU personnel georeferenced the classified images to existing aerial photography.

USLE C factors were derived from a variety of sources and are listed in Table 2.1.1. A final map of USLE C factor for the study area is given in Figure 2.1.2.

LS Factor

LS factor was estimated from topographic data. Moore and Wilson (1992) approximated the LS factor in the RUSLE as:

$$LS = (A_s / 22.13)^{0.6} (\text{Sin}\ \theta / 0.0896)^{1.3}$$

where A_s is the upslope contributing area divided by the width of the pixel and θ is the slope of the pixel. A_s is derived from a flow accumulation (Figure 2.1.3) of the DEM performed in ArcView using Hydrotools 1.0 (Schäuble 2003). Hydrotools includes a multi-path algorithm based on Quinn *et al. (*1991) which produces more realistic flow accumulations than traditional methods. This multi-flow algorithm directs a portion of the flow to all down slope cells, not only to the most down slope cell as done by traditional algorithms. Since RUSLE is intended to predict rill and interrill erosion, we limited the flow accumulation to a maximum of 15 cells, which is equivalent to a maximum flow length of 150 meters.

Pixel slope was also derived from the DEM. A map of the combined LS factor is given in Figure 2.1.4. These data have a resolution equivalent to the original DEM, 1/3 arc second (~10m).

K Factor

The USLE K factor represents soil erodibility. Soil information was given in SSURGO (State Soil Survey Geographic) data provided by the Natural Resources Conservation Service (NRCS). These data are essentially digitized soil survey manuals. The USLE K factor was included in the SSURGO database. These data are natively vector, but were sampled into raster format at the resolution of the DEM (Figure 2.1.5).

R Factor

The rainfall factor was taken as a constant of 120 ft*ton*in/acre*hr*storm for Delaware County, Oklahoma (Haan *et al.*, 1994). Although R factor varies spatially we did not consider it to vary significantly across the study area.

P Factor

The conservation practice factor was assumed to be equal to one, i.e. no conservation practices in effect. Without specific information about what practices were used on which fields within the study area, a uniform conservation practice factor was necessary to prevent biasing the targeting results.

RUSLE Predicted Erosion

RUSLE predicted erosion is given in Figure 2.1.6. Erosion estimated ranged from 0.0 to 275 tons per acre with an average of 0.65 tons/acre for the study area. High rates of erosion were not realistic and were primarily due to errors in the input data in isolated cells. For this reason erosion was limited to 25 tons/acre. For the purpose of targeting, absolute rates are less important than the relative differences between cells.

Table 2.1.1 USLE C factors for landcovers in the study area.

Landcover	USLE Crop Factor	Notes
High Biomass Pasture[2]	0.003	Grass 95% cover
Low Biomass Pasture[2]	0.035	50% tall weeds over 60% grass cover
Rangeland[2]	0.013	25% brush over 80% grass cover
Urban[2]	0.042	Grass 60% cover
Wheat/beans[1]	0.25	Estimated from soybeans and winter wheat.
Forest[1]	0.0001	
Bare[2]	0.20	20% Grass cover
Water	0.0	Not Applicable
Stream[2]	0.003	50% Brush, 95% ground cover

1) C. T. Haan, Barfield, B.J., and J.C. Hayes. 1994. Design hydrology and sedimentology for small catchments. New York: Academic Press.
2) 1977, Procedure for computing rill and interrill erosion on project areas, SCS (NRCS) technical release 51.

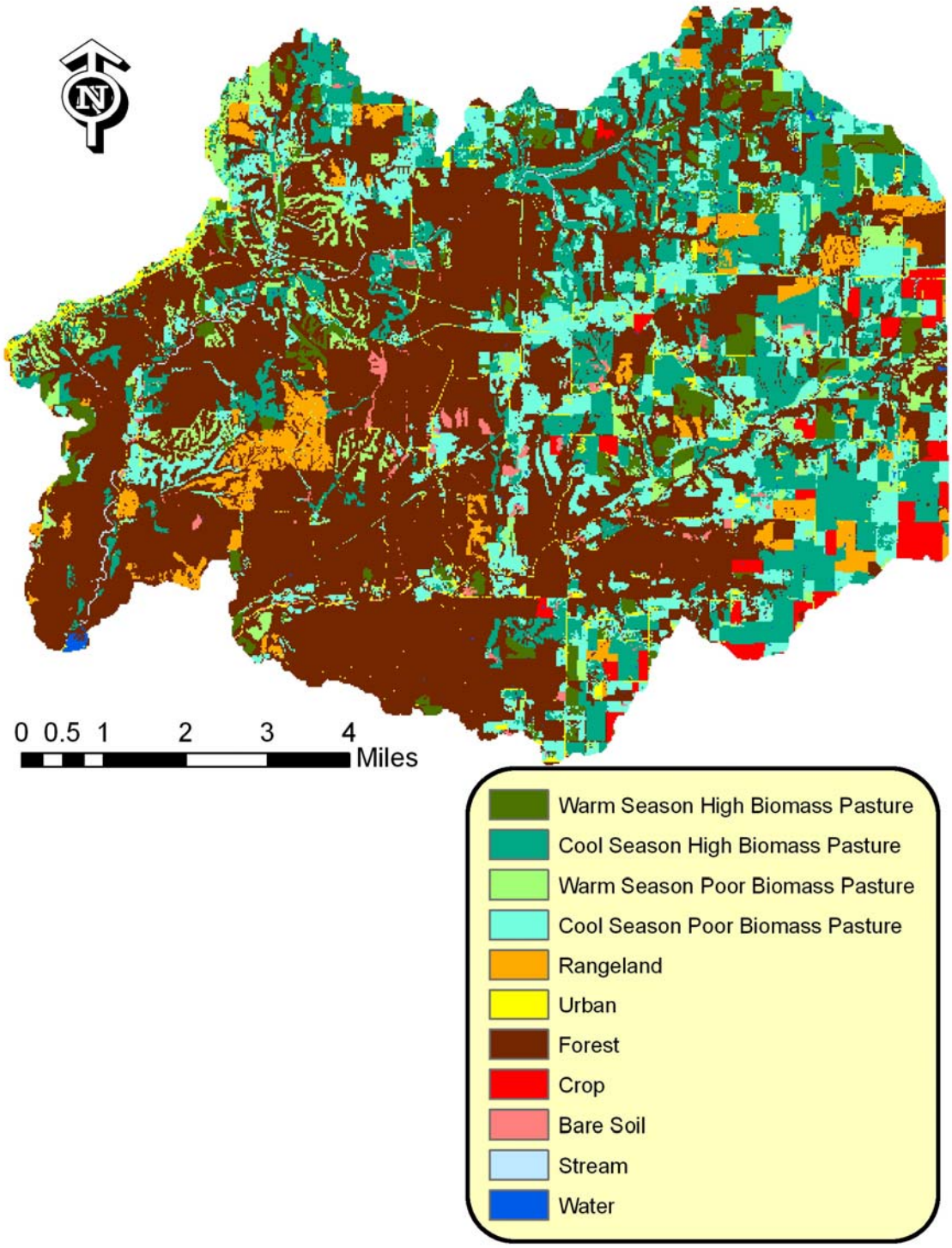

Figure 2.1.1 IKONOS derived landcover.

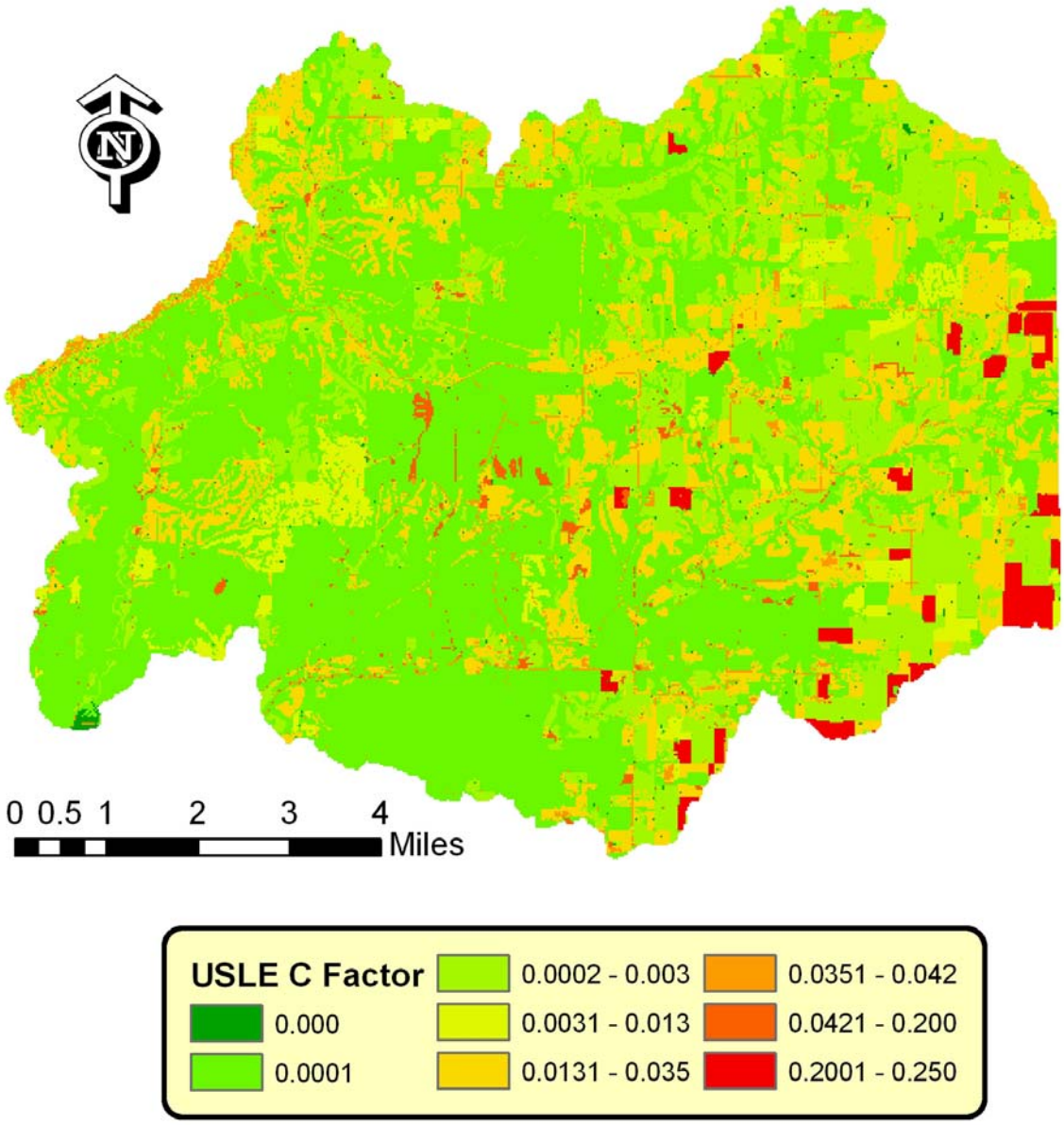

Figure 2.1.2 Universal Soil Loss Equation (USLE) C factors based on Landcover.

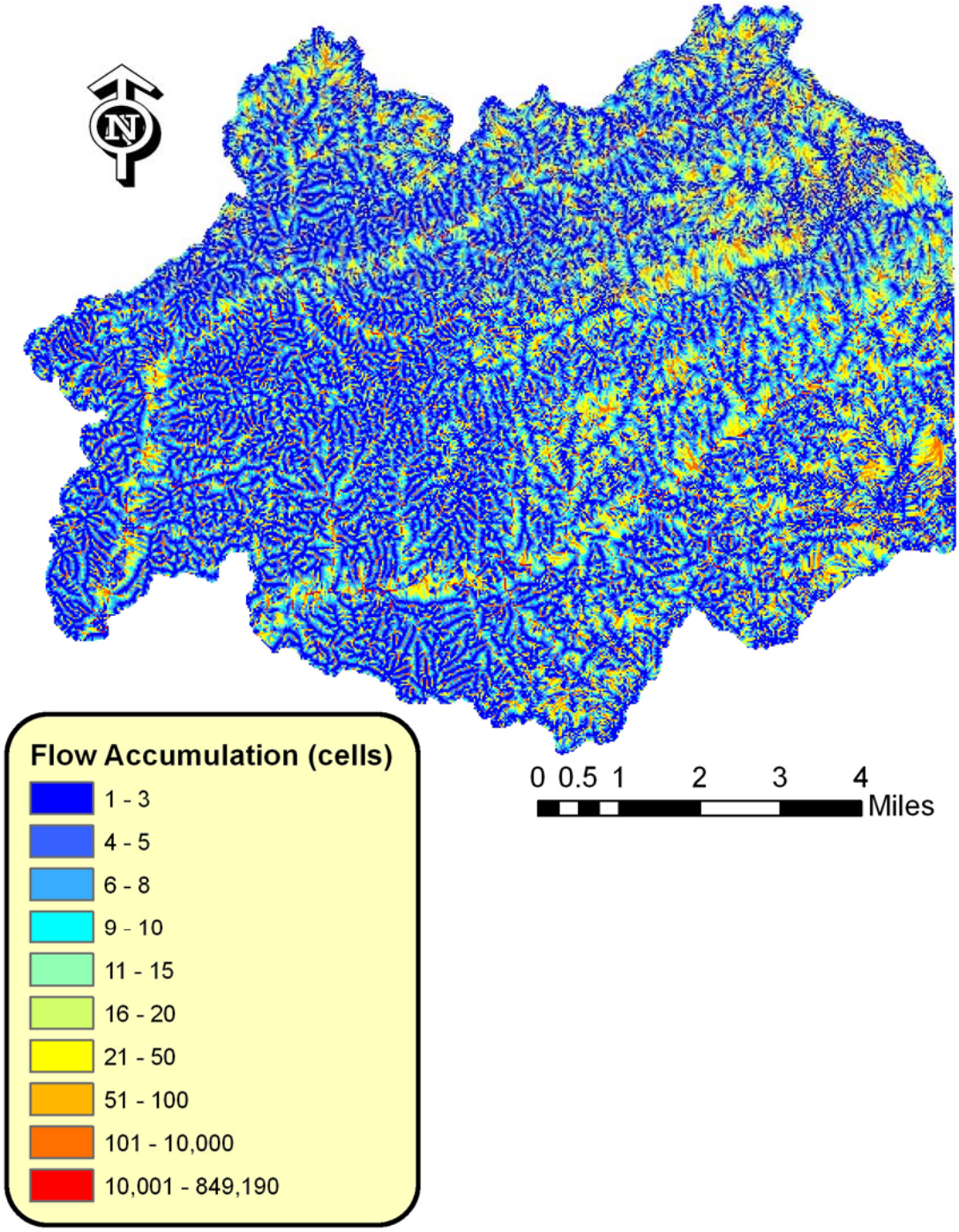

Figure 2.1.3 Flow accumulation used to estimate flow lengths for Revised Universal Soil Loss Equation (RUSLE) LS factor.

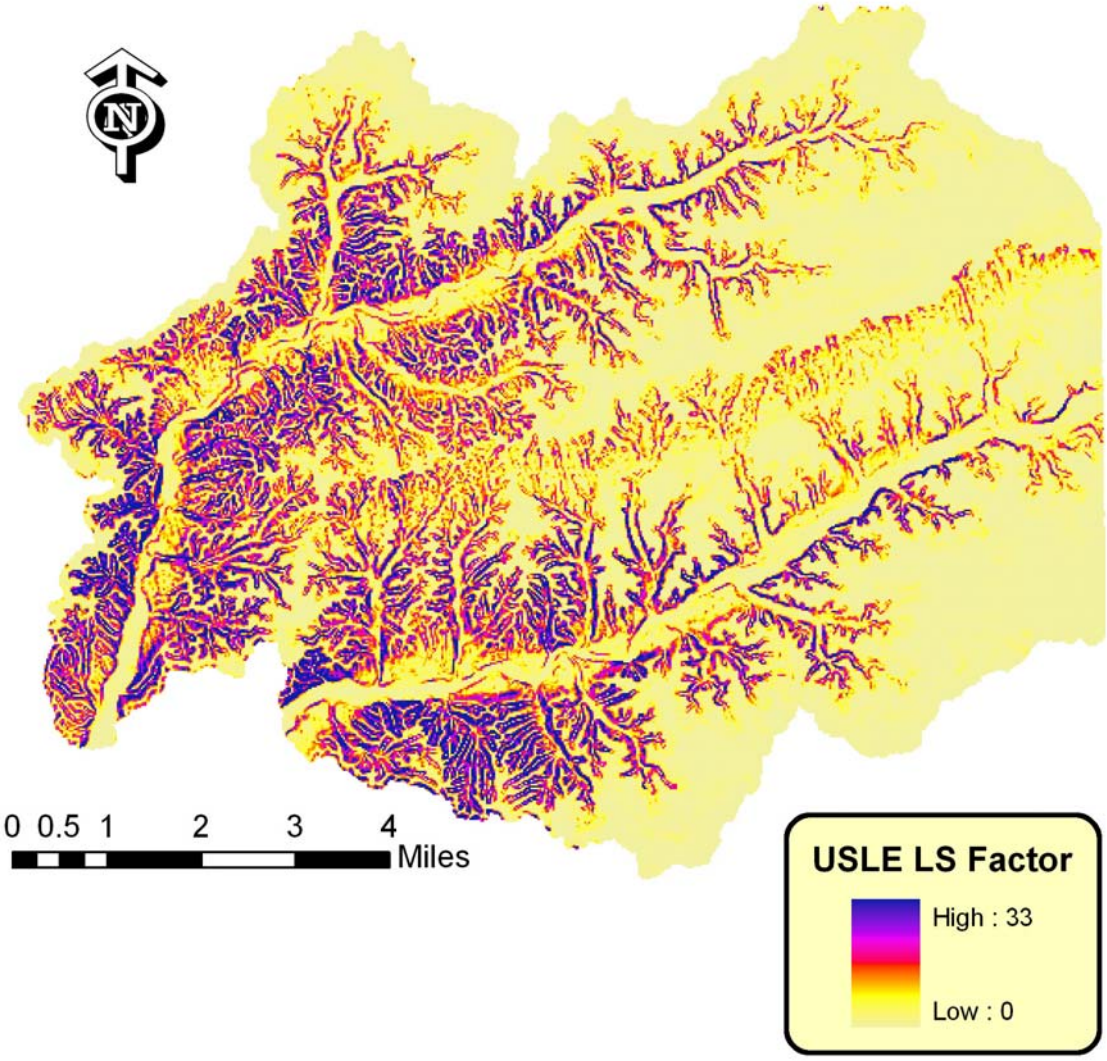

Figure 2.1.4 Revised Universal Soil Loss Equation (RUSLE) LS factor used to predict gridcell erosion.

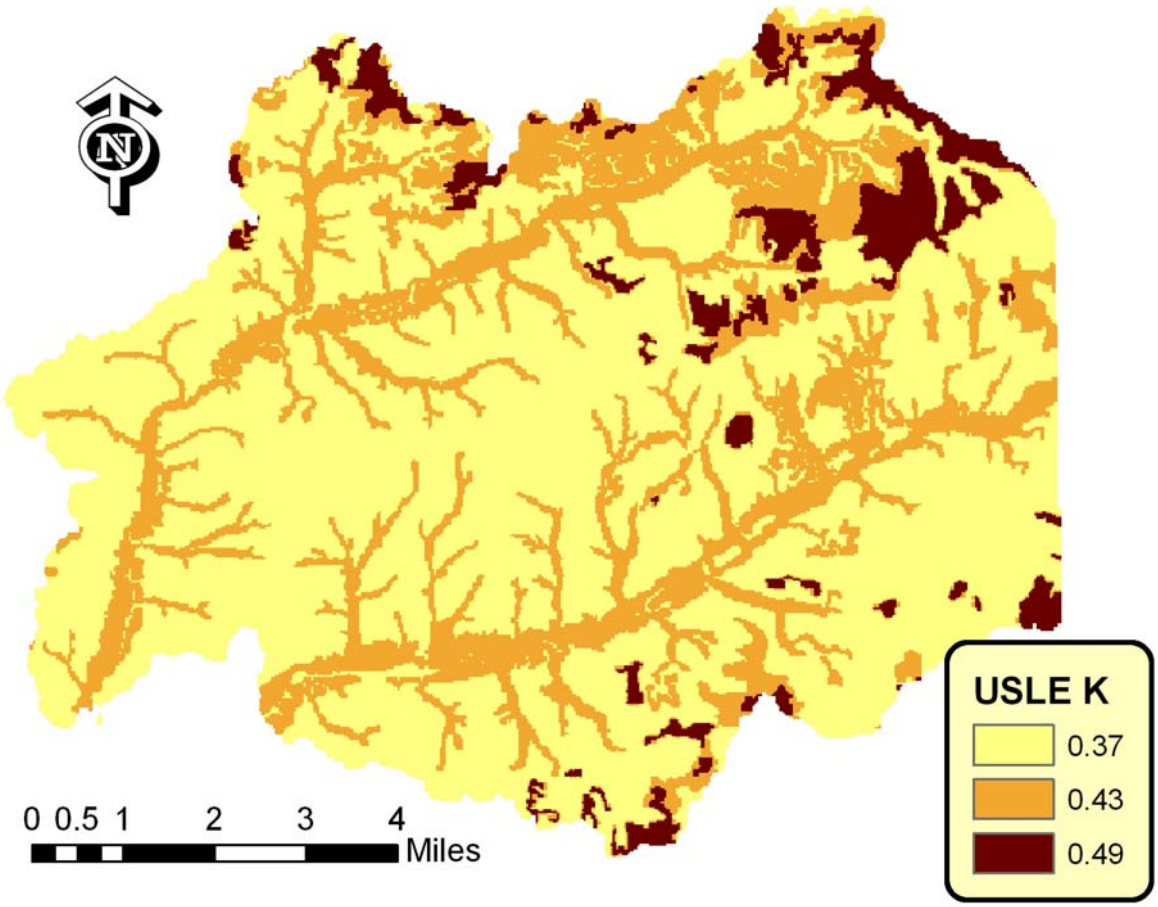

Figure 2.1.5 Universal Soil Loss Equation (USLE) K factor (English units) used to predict gridcell erosion, derived from State Soil Geographic (SSURGO) data.

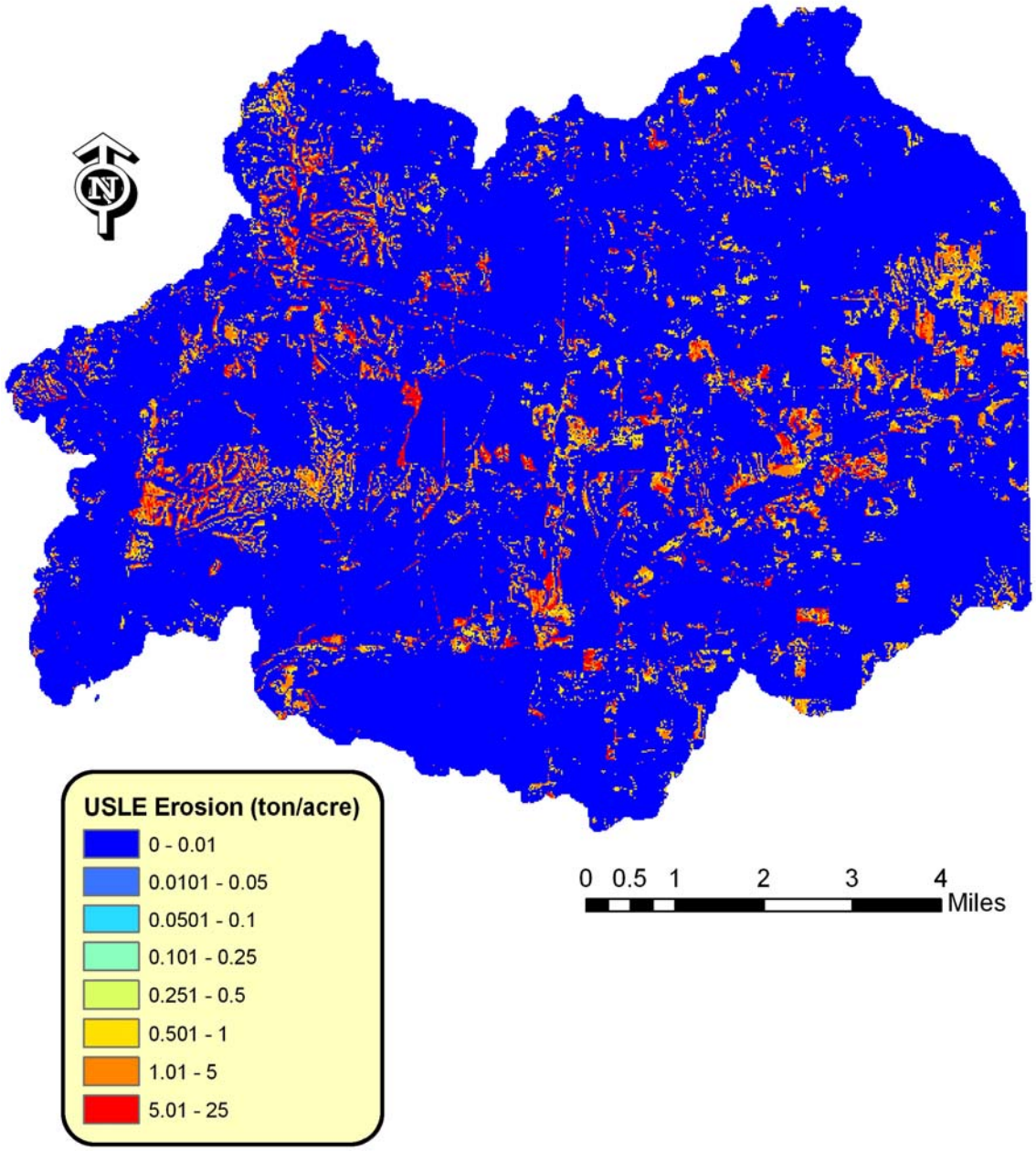

Figure 2.1.6 Universal Soil Loss Equation (USLE) predicted gridcell erosion.

(2.2) Extrapolated SWAT Runoff and Soluble Phosphorus

In pasture systems with little erosion, most phosphorus is transported in soluble forms. The amount of soluble phosphorus lost from a field is primarily a function of weather, land use, management, and soils. It is difficult to estimate the quantity of soluble phosphorus lost from every gridcell in the basin. Models such as SWAT can be used, but it is difficult to run SWAT on a gridcell basis, and out of the scope of this project. As a surrogate for true gridcell model predictions, estimates by landcover and soil were interpolated from SWAT model results by Storm *et al.* (2005) in the neighboring Spavinaw Creek Basin. SWAT model predictions were summarized by hydrologic soil group and landcover (Table 2.2.1). Gridcells within the original GIS data with the same hydrologic soil group and landcover were assigned runoff and soluble phosphorus yields from Table 2.2.1. Because the original landcover data did not specify littered or non-littered pasture, the average of three scenarios was used. The three scenarios were pasture with litter, pasture with commercial nitrogen, and pasture with no fertilization of any kind. If litter pastures locations and their boundaries were known, this information could be included.

Runoff and soluble phosphorus yields vary widely across the study area (Figure 2.2.1 and 2.2.2). Both runoff volume and soluble phosphorus yield are higher in the upland portions of the study areas. The areas have different soils, as illustrated in Figure 2.2.3, with higher runoff potential in the upland areas. Fraction of rock, silt, and clay are given in Figures 2.2.4 to 2.2.6, illustrating the differences in soil properties across the study areas.

Table 2.2.1 SWAT predictions summarized by landcover and hydrologic soil group by Storm *et al.* (2005).

Land Cover	Hydrologic Soil Group								
	B			C			D		
	Surface Runoff (mm)	Soluble P (kg/ha)	Total P (kg/ha) .	Surface Runoff (mm)	Soluble P (kg/ha)	Total P (kg/ha) .	Surface Runoff (mm)	Soluble P (kg/ha)	Total P (kg/ha) .
Cultivated	118	0.193	0.726	218	0.386	2.448	257	0.488	2.822
Bare	146	0.248	0.597	222	0.263	0.912	255	0.380	1.498
Forest	18	0.001	0.003	110	0.004	0.018	142	0.004	0.047
Range	42	0.010	0.012	139	0.026	0.037	196	0.052	0.068
Stream	50	0.002	0.006	147	0.004	0.010	197	0.005	0.010
Urban	118	0.695	0.773	193	1.015	1.172	223	1.230	1.429
Water	0	0.000	0.000	0	0.000	0.000	0	0.000	0.000
Litter-Good Condition Warm Season Pasture	45	0.685	0.708	119	1.880	2.008	152	2.576	2.780
Litter-Good Condition Cool Season Pasture	50	0.752	0.787	128	1.984	2.174	173	2.823	3.090
Urea-Good Condition Warm Season Pasture	43	0.150	0.165	114	0.444	0.519	153	0.599	0.713
Urea-Good Condition Cool Season Pasture	48	0.154	0.164	124	0.394	0.445	169	0.577	0.650
No Fert-Poor Condition Warm Season Pasture	142	0.326	0.757	227	0.556	1.807	251	0.606	2.241
No Fert-Poor Condition Cool Season Pasture	152	0.399	0.665	232	0.610	1.351	268	0.758	1.744
No Fert-Good Condition Warm Season Pasture	41	0.093	0.108	113	0.266	0.349	147	0.349	0.486
No Fert-Good Condition Cool Season Pasture	48	0.070	0.081	125	0.182	0.234	166	0.280	0.356
Good Condition Warm Season (Average)*	43	0.310	0.327	115	0.863	0.958	151	1.175	1.326
Good Condition Cool Season (Average)*	49	0.325	0.344	126	0.854	0.951	169	1.226	1.365

* Average of all good condition pasture

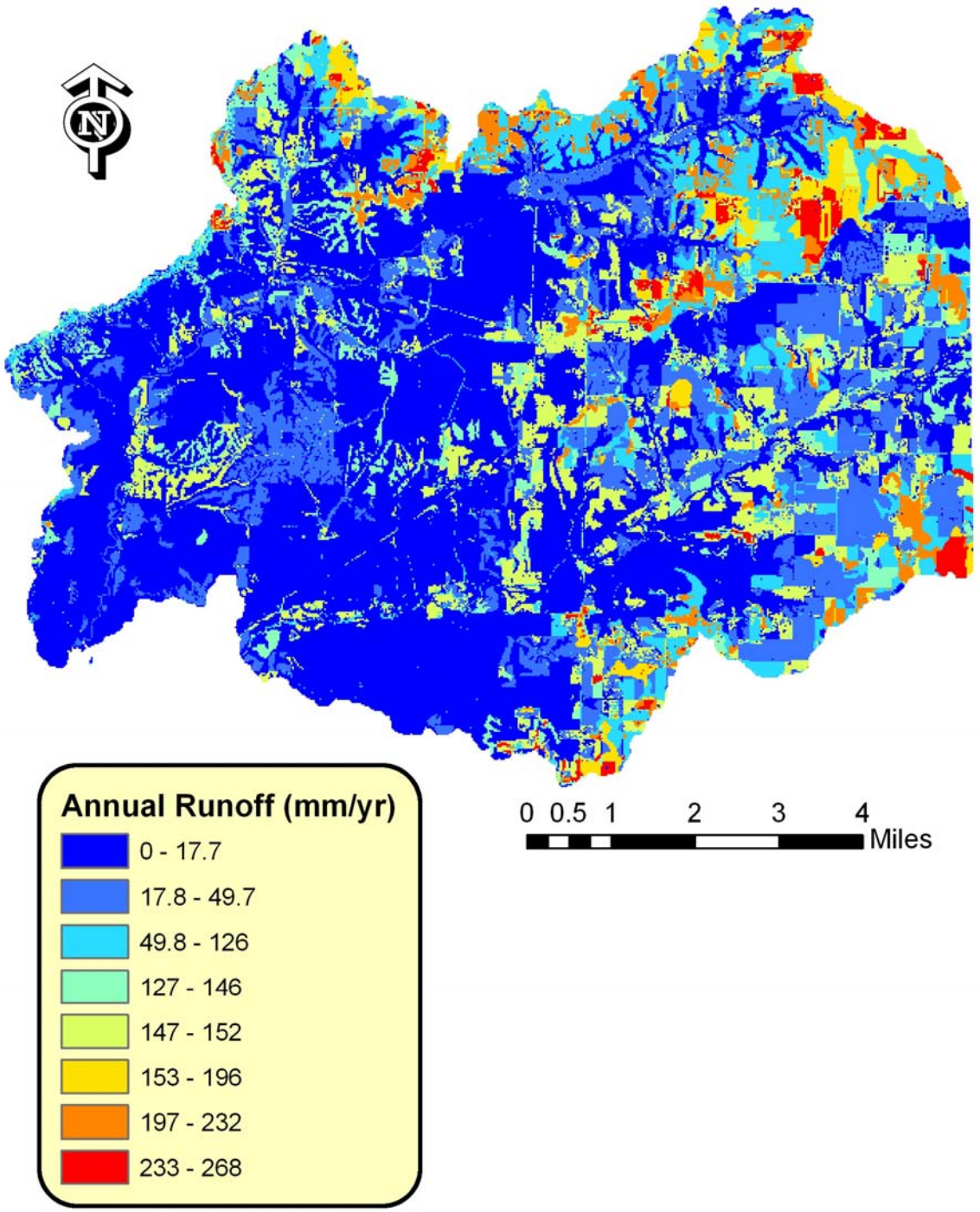

Figure 2.2.1 Gridcell annual runoff volume extrapolated from SWAT model prediction of the Spavinaw Creek Basin (Storm *et al.*, 2005).

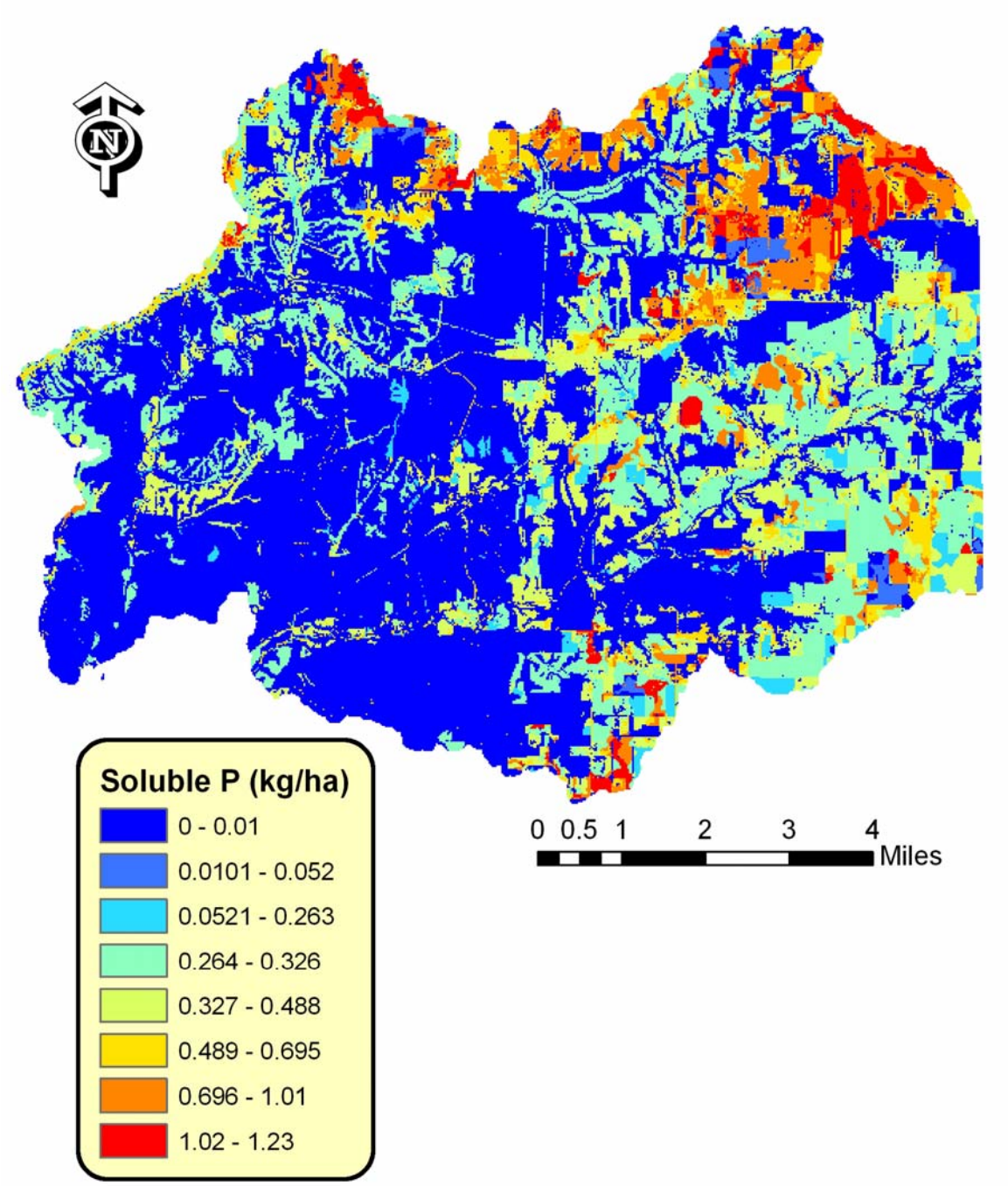

Figure 2.2.2 Gridcell annual soluble phosphorus load extrapolated from SWAT model prediction of the Spavinaw Creek Basin (Storm *et al.,* 2005).

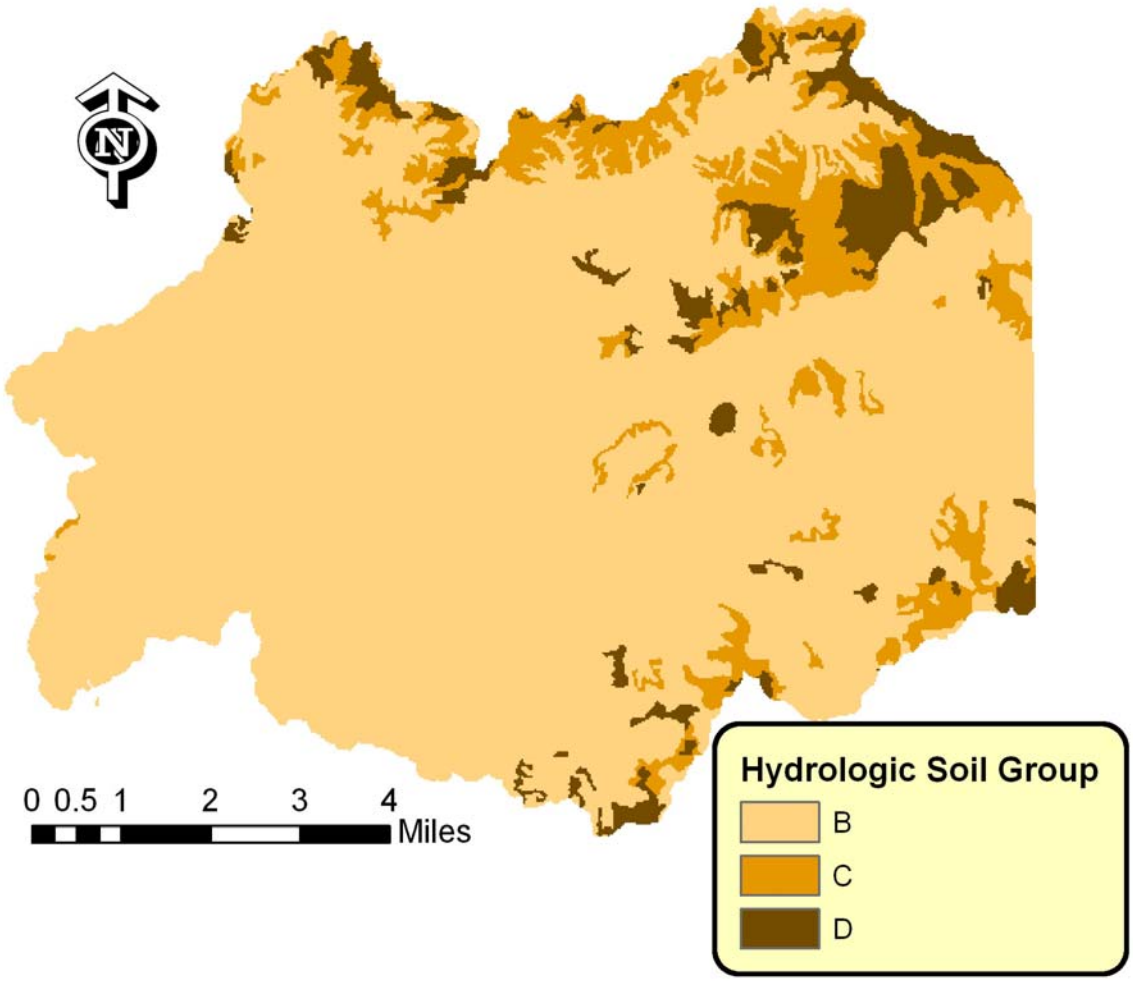

Figure 2.2.3 Hydrologic soil group derived from State Soil Geographic (SSURGO) data.

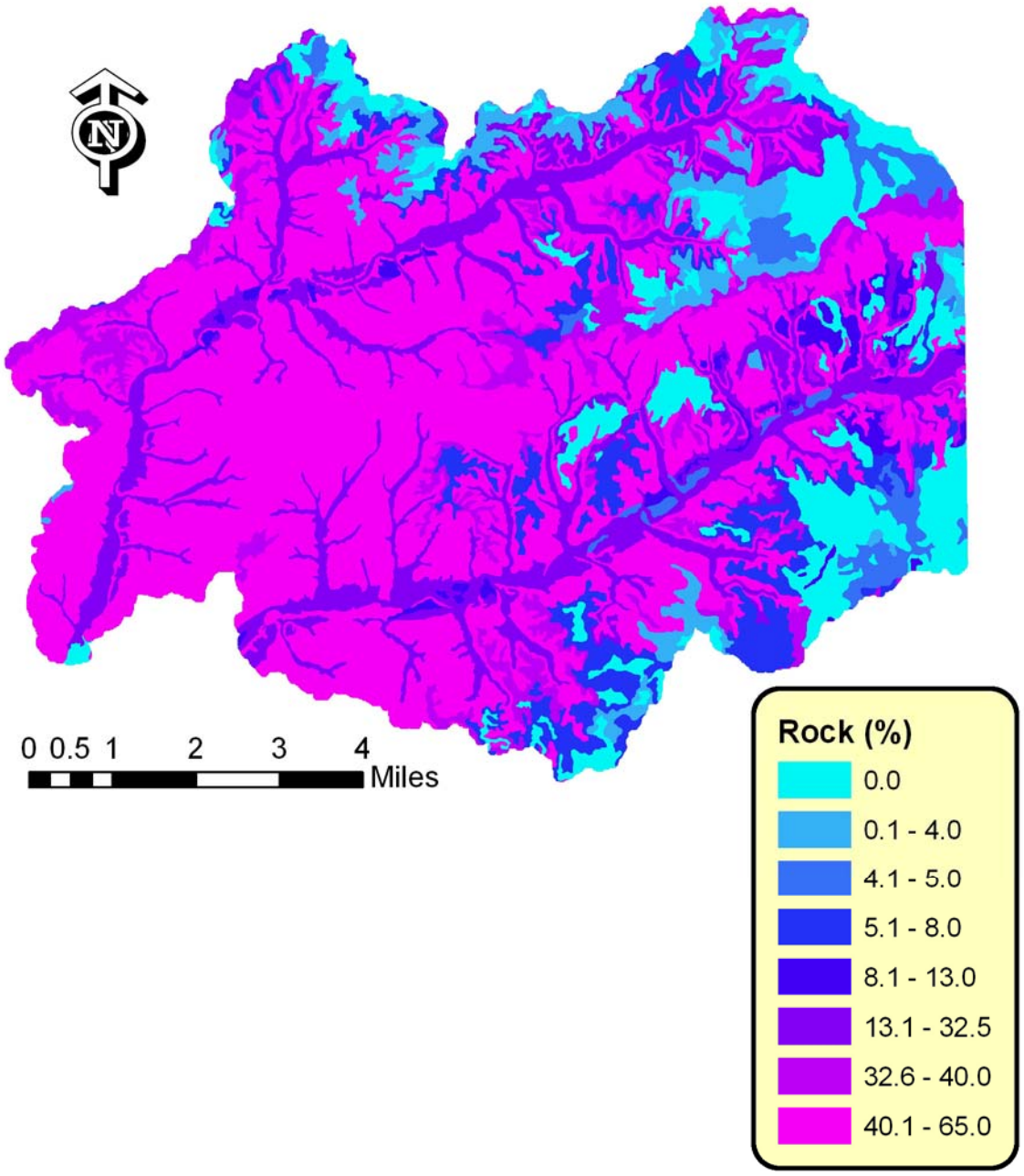

Figure 2.2.4 Fraction of rock in the surface soil layer across the study area. Derived from State Soil Geographic (SSURGO) data.

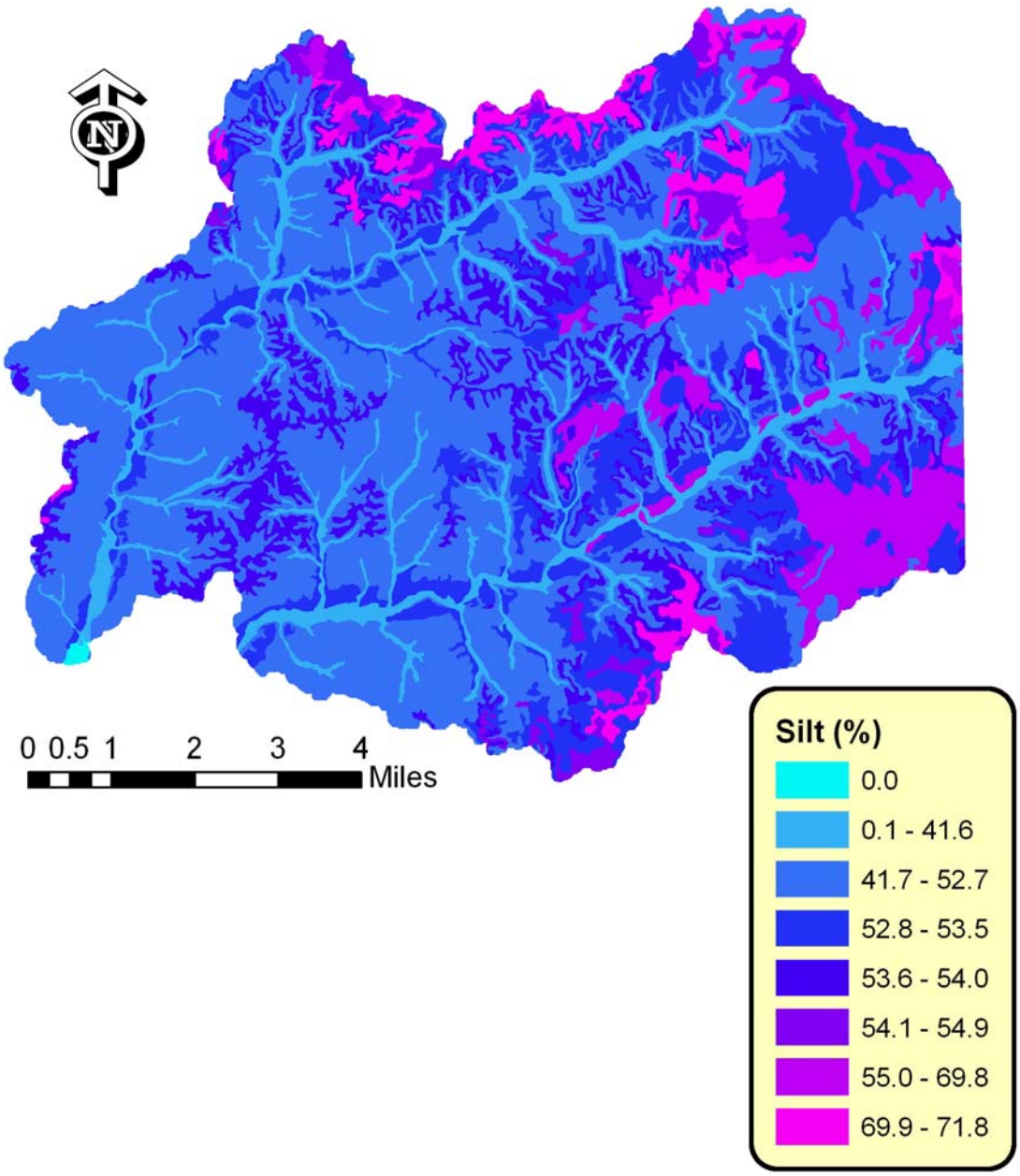

Figure 2.2.5 The fraction of silt in the surface soil layer across the study area. Derived from State Soil Geographic (SSURGO) data.

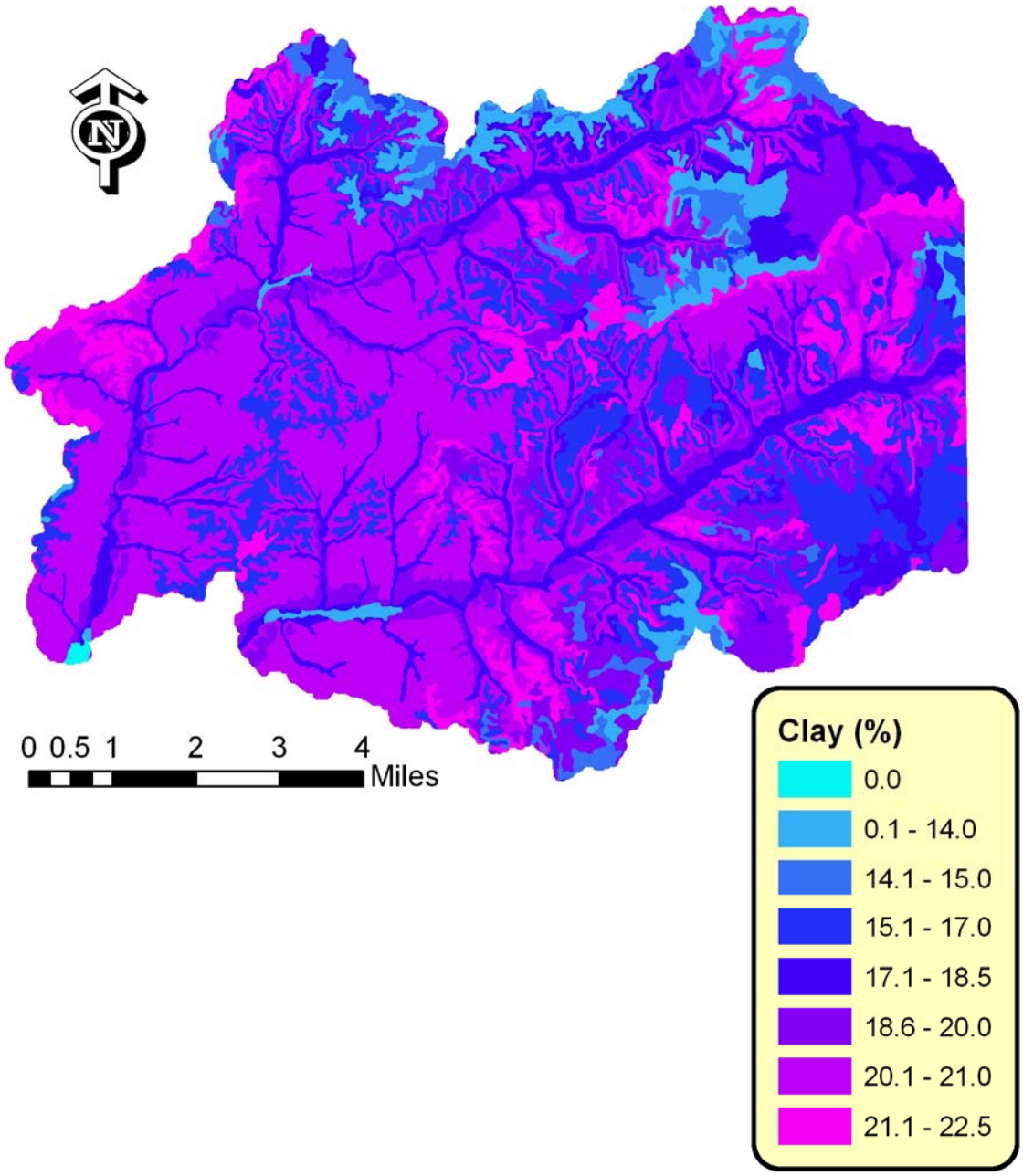

Figure 2.2.6 The fraction of clay in the surface soil layer across the study area. Derived from State Soil Geographic (SSURGO) data.

(2.3) Flow Accumulation

The RUSLE gridcell sediment, SWAT extrapolated runoff volume, and soluble phosphorus yield provided estimates of the production of sediment and nutrients, but not how and where these are transported to the stream. Flow accumulation provided estimates of how water moves across the land surface to streams and rivers. In order to evaluate a site for riparian performance we must know how much water, sediment, and nutrients enter a particular riparian zone. A riparian buffer cannot filter water which does not pass through it. However, if the flow is too concentrated it will channelize, the riparian buffer will be bypassed and will not function properly.

Flow accumulation can be used to determine the amount of runoff flowing through any given cell of a DEM. Traditional flow accumulations assume all gridcells produce one unit of runoff, and are therefore a measure of drainage area, not flow as the name implies. An example of traditional flow accumulation is given in Figure 2.3.1. One weakness of the traditional flow accumulation is that the entire flow accumulated in a cell is transferred to the most down slope adjacent cell, even if other adjacent cells are also down slope. This is not realistic using a DEM based on the average elevation for a 10*10 meter cell. It is likely that parts of each 10 meter cell will pass flow down slope to multiple cells. This weakness is overcome by using the ArcView Extension Hydrotools 1.0 (Schäuble, 2003). Hydrotools has a multi-path algorithm based on Quinn *et al*. (1991), which produces more realistic flow accumulations by routing flow to all down slope cells based on the elevation difference. Once the flow accumulation reaches 500 cells, the traditional method of routing all flow to the most down slope cell is used. The multi-path algorithm was applied to the study area and is shown in Figure 2.3.2.

Estimates of erosion, runoff volume and soluble phosphorus were made in sections 2.1 and 2.2 for each 10 meter gridcell in the study area. How these were transported to the stream determine in part the effectiveness of a riparian buffer. Most flow accumulation algorithms assume one unit of runoff per gridcell; however Hydrotools 1.0 can utilize a weighting grid to allow an estimated runoff for each gridcell to be utilized. This function was used to produce flow accumulation of runoff volume, sediment, and soluble phosphorus load. This procedure ignored losses due to deposition, even though significant. Before accumulation the runoff volume, sediment and soluble phosphorus load grids were normalized such that the average gridcell value was 1.00 to make all accumulation grids relative in magnitude. The results are given in Figures 2.3.3 to 2.3.5. The sediment accumulation grid had higher values in steeper sloping areas and erosive landcovers. Runoff volume accumulation was higher in the B and C hydrologic group soils in the eastern and north eastern portions of the study area. Soluble phosphorus accumulation was similar to that of runoff volume.

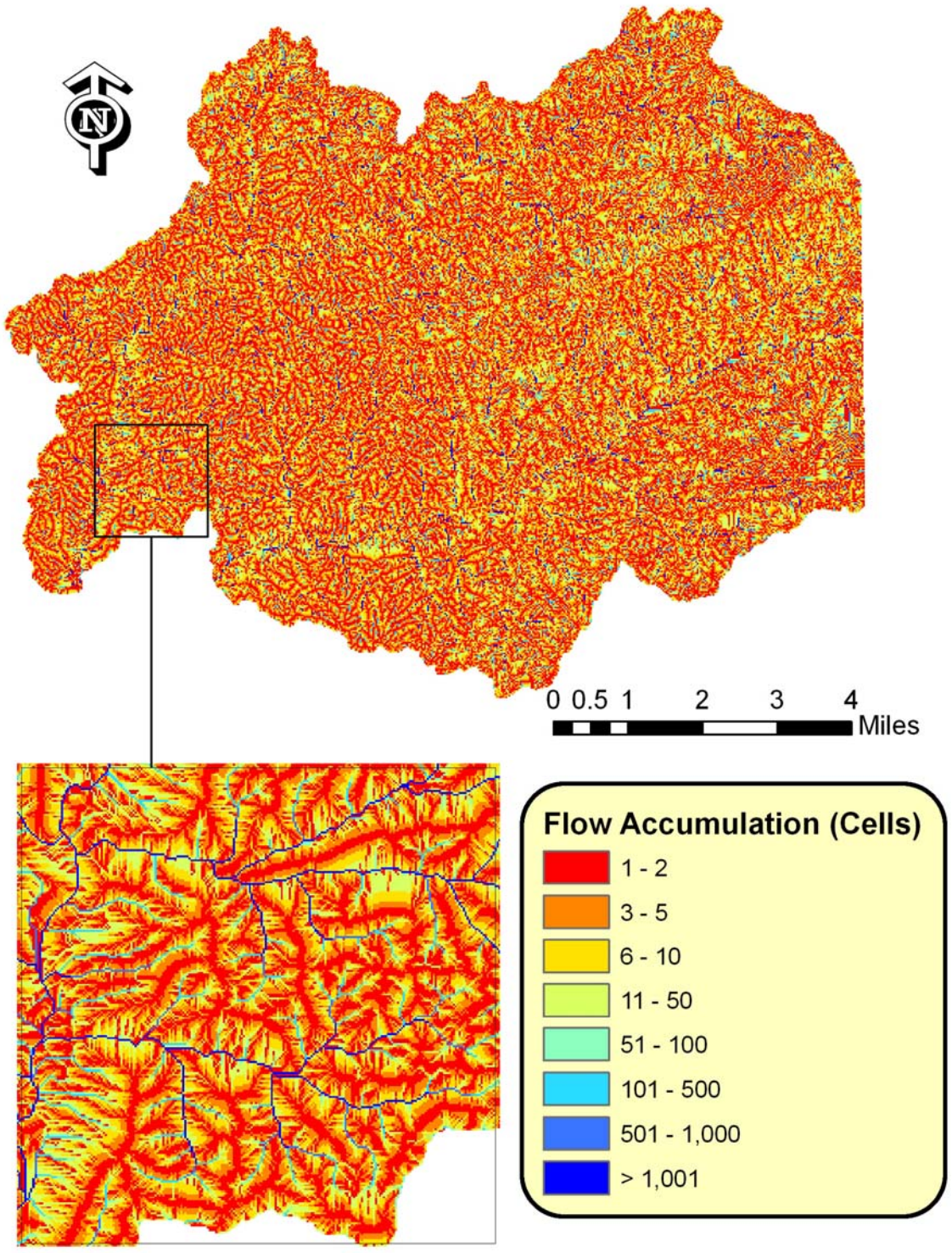

Figure 2.3.1 Traditional flow accumulation in the study area.

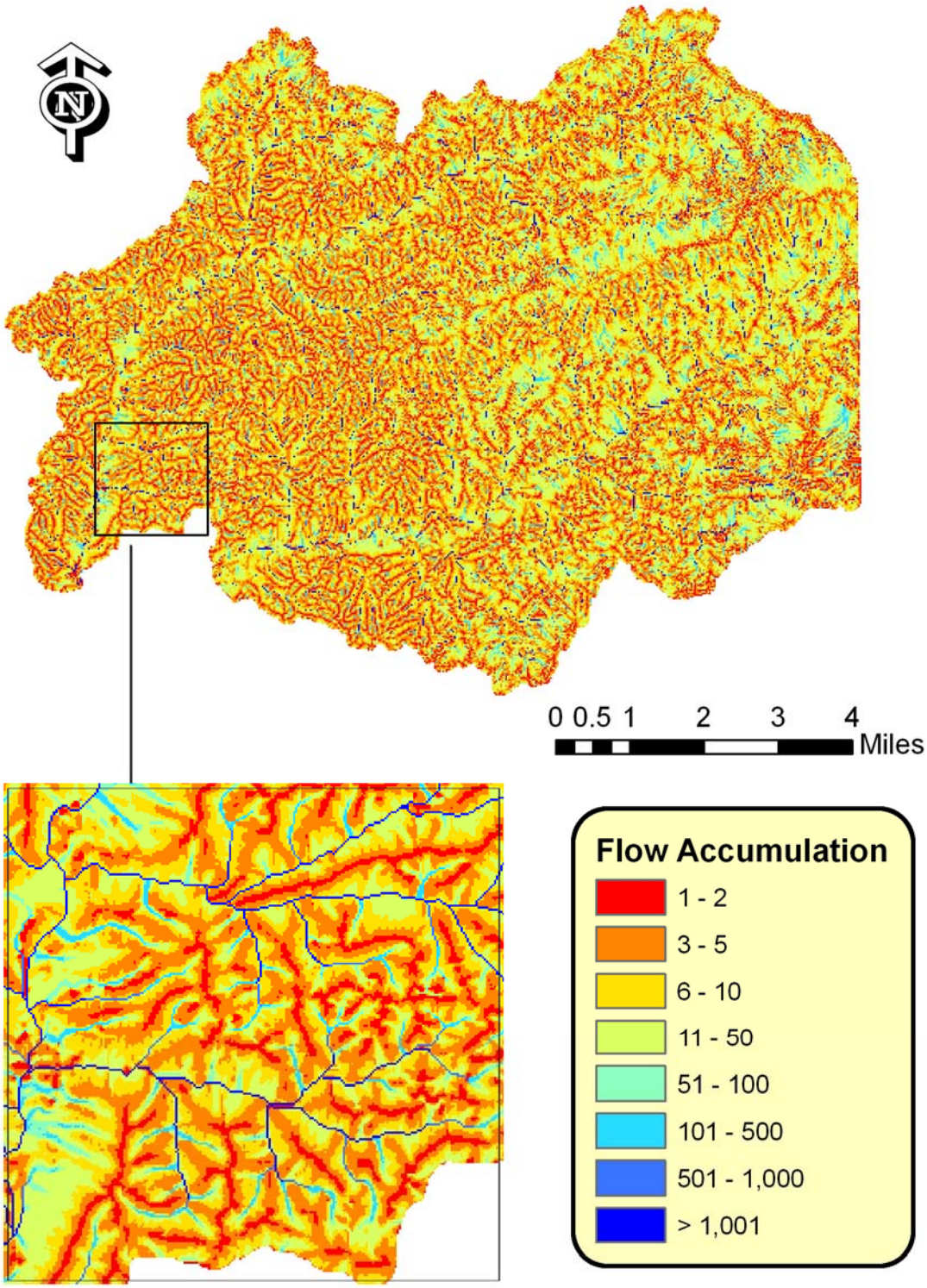

Figure 2.3.2 Flow accumulation in the study area using multi-path algorithm.

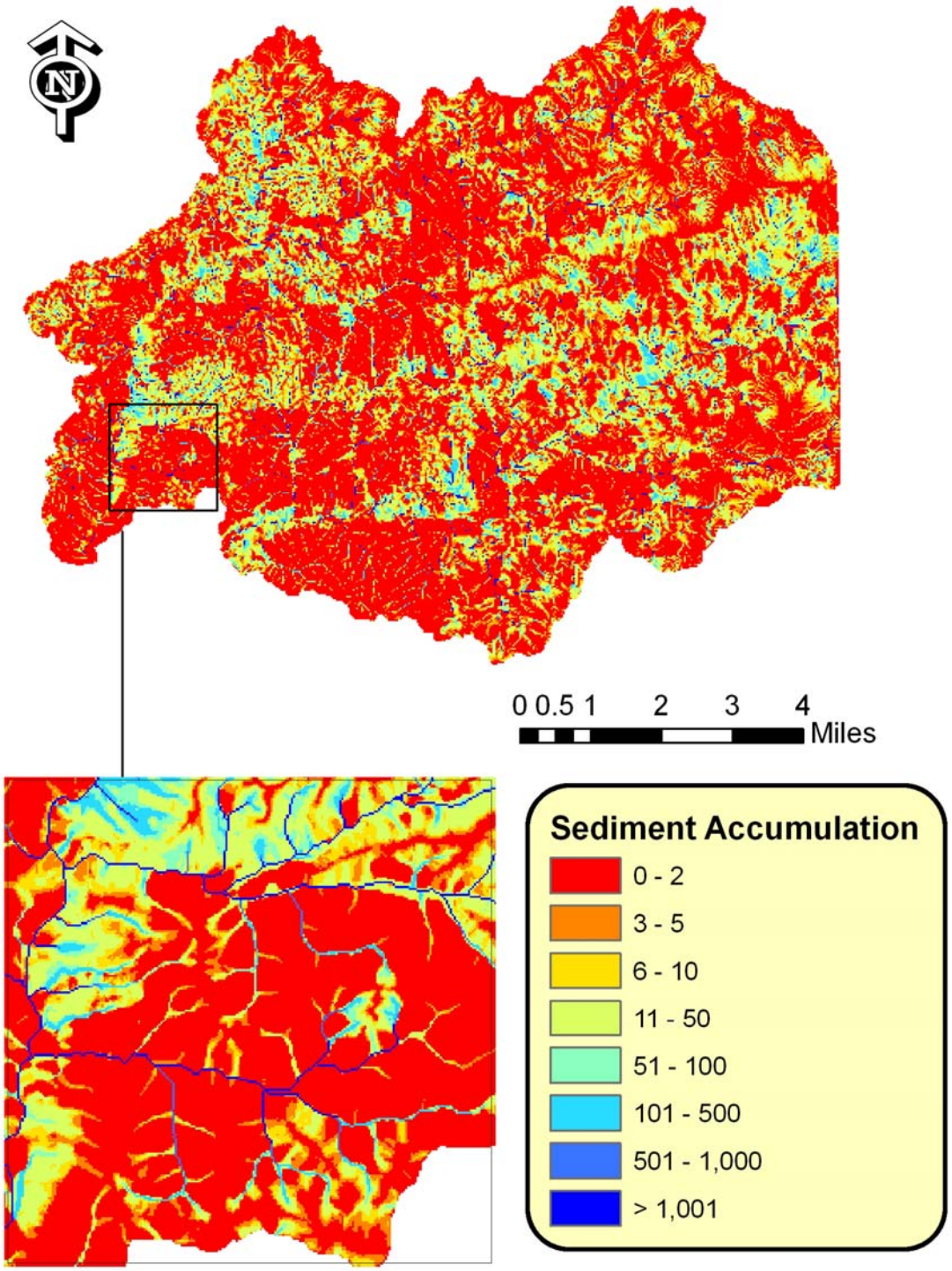

Figure 2.3.3 Sediment accumulation in the study area using multi-path algorithm and relative erosion as predicted by the Revised Universal Soil Loss Equation (RULSE). Does not account for sediment deposition.

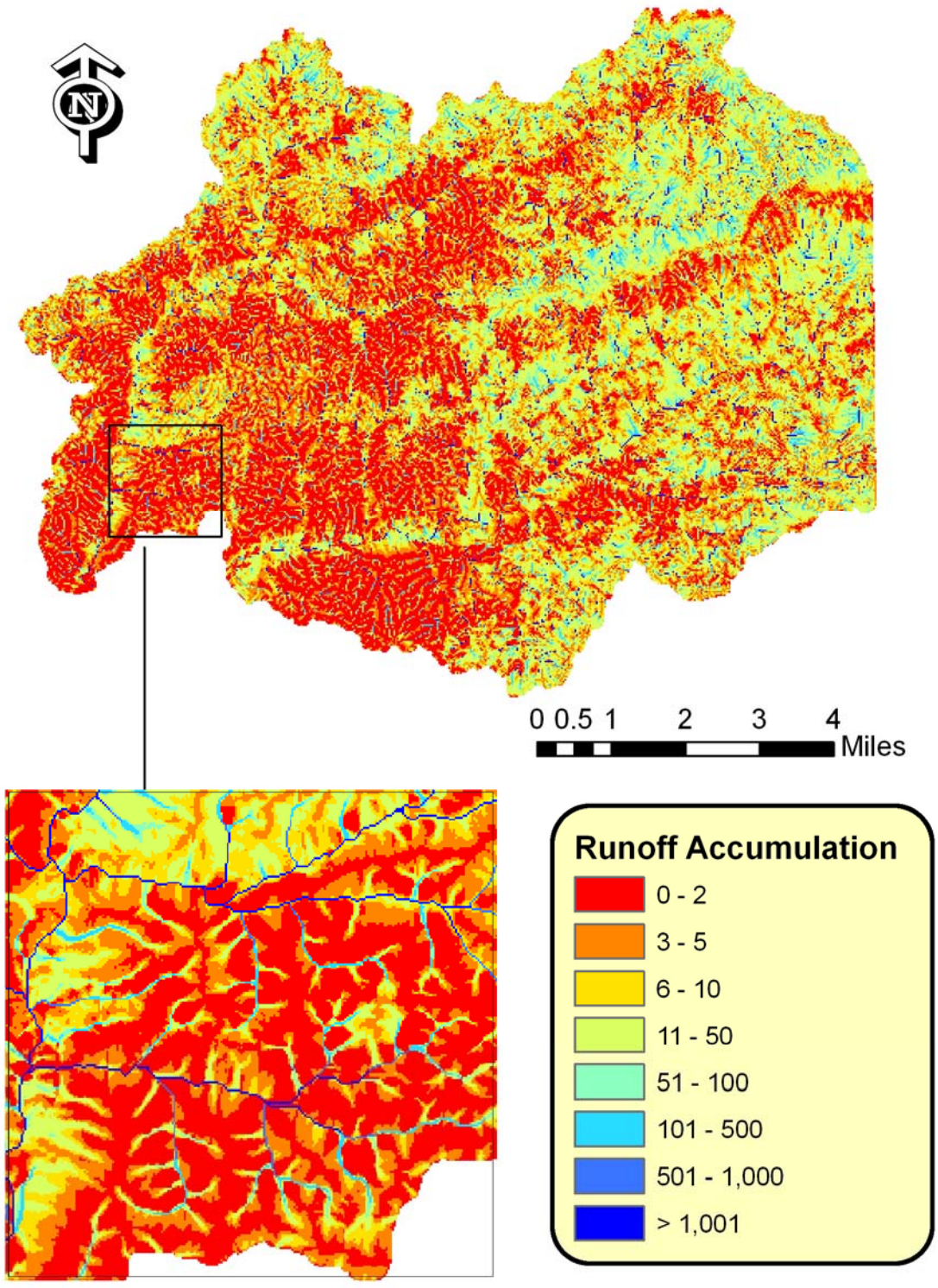

Figure 2.3.4 Runoff accumulation in the study area using multi-path algorithm and relative surface runoff as extrapolated from Soil and Water Assessment Tool (SWAT) predictions in neighboring Spavinaw Creek.

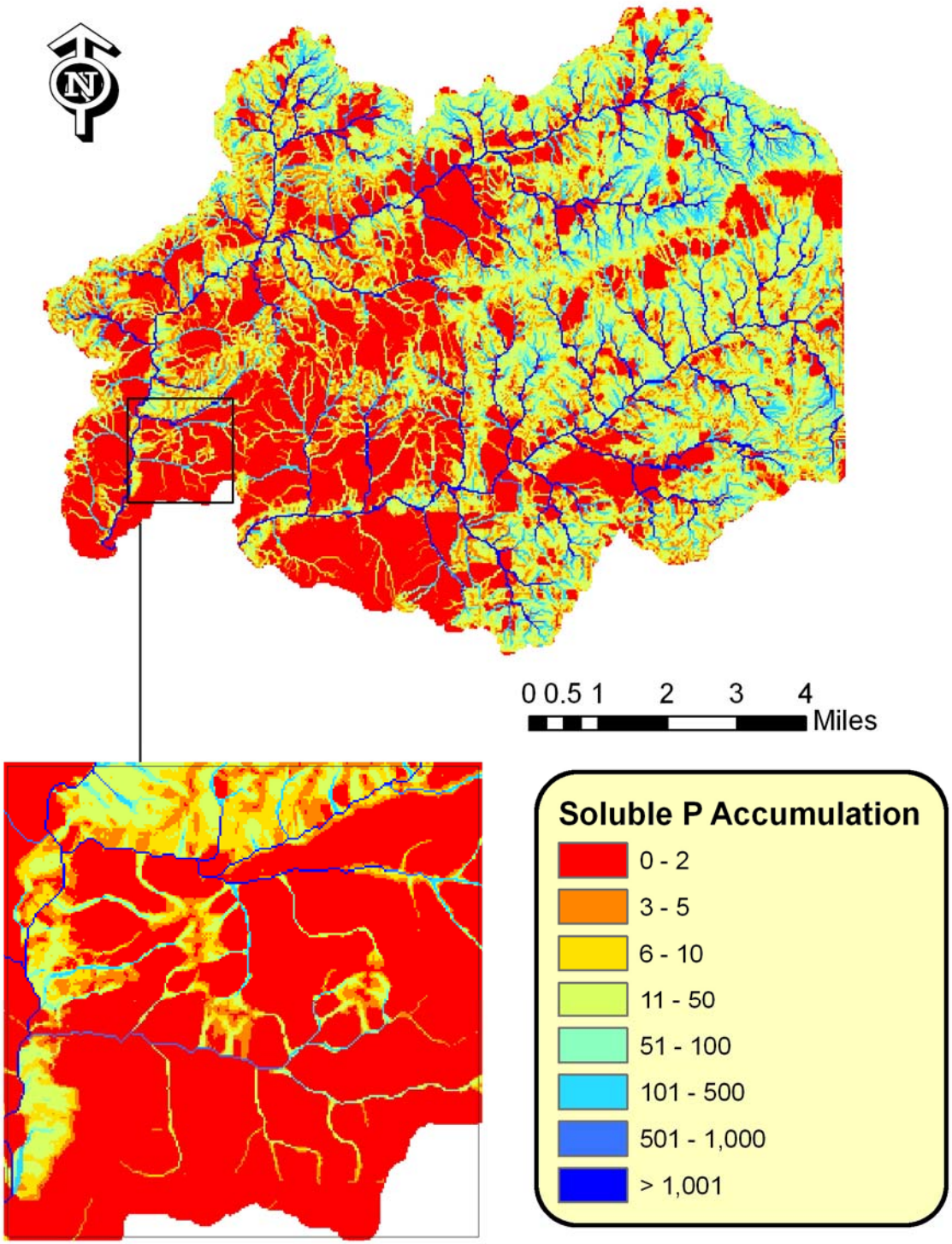

Figure 2.3.5 Soluble P accumulation in the study area using multi-path algorithm and relative soluble phosphorus yield as extrapolated from Soil and Water Assessment Tool (SWAT) predictions in neighboring Spavinaw Creek.

(2.4) Stream Shape and Sinuosity

Stream shape and sinuosity influences the distribution of erosive energy within the stream channel. Energy is concentrated on the outside of each meander resulting in an area of more active stream bank erosion known as a cut bank. A Point bar is an area of deposition occurring on the inside of each meander where flow velocity is reduced. As sediment is eroded from cut banks and deposited in point bars meanders may migrate outward or translocate in a downstream direction, consuming riparian area and reducing the available buffer.

Complex flow models can predict the migration of streams (Furbish 2001). For the purposes of targeting, it is not necessary to quantitatively estimate cut bank migration or stream bank erosion. In lieu of a model, we chose to identify stream segments with tight curvatures as potential sites with increased bank erosion and stream bank instability. In particular the outside of tight curvatures were considered a higher priority, and the inside of the curve was lower, and straight segments were neutral.

Data

Highly accurate stream GIS data were important. Streams were derived from the Digital Elevation model using flow accumulation. Streams were defined using a minimum contributing area of 50 ha to form a stream. We considered using the National Hydrography Dataset (NHD) (Figure 2.4.1) to define streams within the study area; however there were significant discrepancies between the two stream networks. Due to the extensive use of flow accumulations in this project, we elected to use streams derived from the DEM to ensure proper overlay between the curvature based and the flow accumulation based factors. This issue should be addressed in future projects. Visual inspections of smaller streams using aerial photography indicated errors in both NHD and DEM derived streams, the best dataset was not clear. NHD was created by the U.S. Environmental Protection Agency (EPA) and the U.S. Geological Survey (USGS) by combining USGS digital line graph (DLG) hydrography files and USEPA Reach File (RF3), and is not directly linked to elevation data, hence the discrepancies between datasets.

Processing

Suitable tools to identify curvature within GIS stream coverage were not currently available. The methods used to quantify curvature used in this project were rather crude. It was certainly possible to create better programs, but it would have required writing complex Avenue or Visual Basic for Applications software to directly report this information from the GIS. This was beyond the scope of this project, but may be necessary in future implementations of this methodology. The methods presented here were based on simplifying the stream network to straight segments, then estimating the angle between each segment and the two connecting segments based on buffer areas. The steps are listed below:

1) The stream network was generalized into straight segments using an Arcview 3.x user extension Point and Polyline tools V1.2 (Alsleben 2001) using a tolerance of 21 meters (~2 DEM grid cells). The complexity of the stream network was reduced as a requirement of this method. A visual comparison between the generalized and original data is given in Figure 2.4.1, and below:

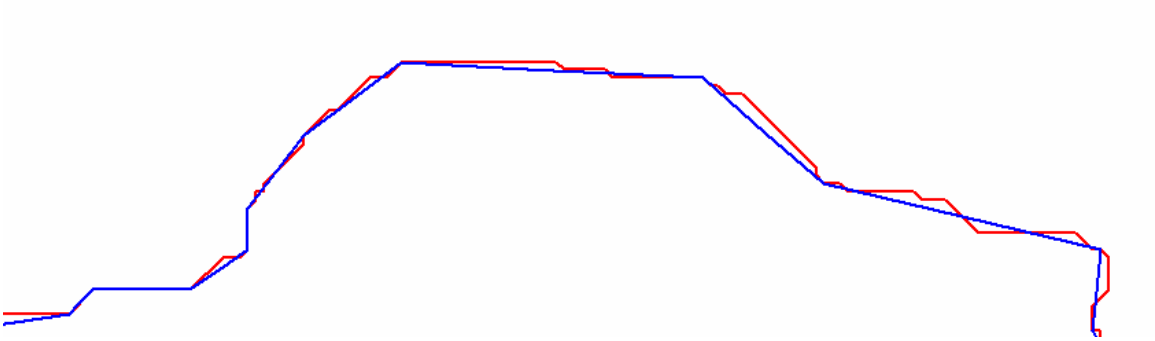

2) The generalized stream data were converted from a connected network to simple unconnected line segments using Point and Polyline tools V1. Each segment was again broken at it midpoint. See the example below, each color represents a separate entity.

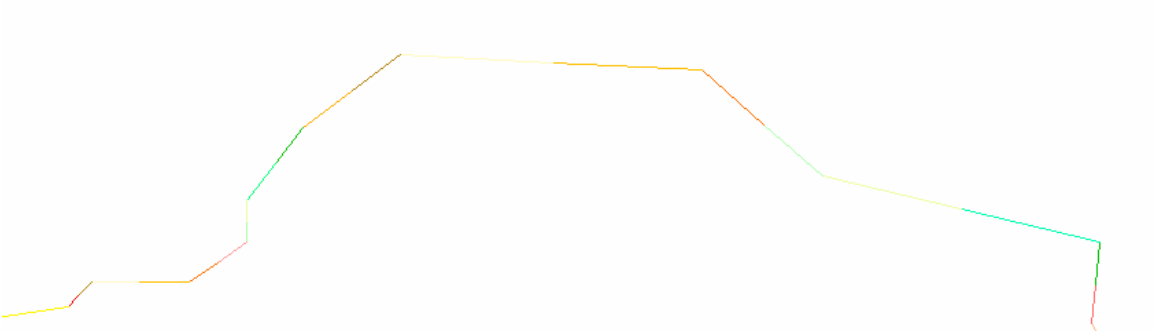

3) The length of each individual segment was added to the table, and each segment was buffered by 50 meters. Each buffer was an independent polygon. The attribute information from the original segment was retained in the buffers attribute table.

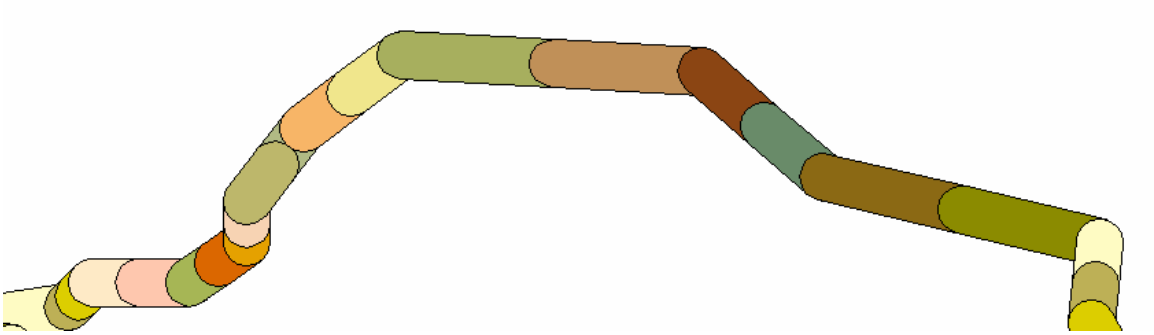

4) The buffered segments were split by the stream network to create separate buffers on each side of the stream for each segment. The area of each buffer was calculated.

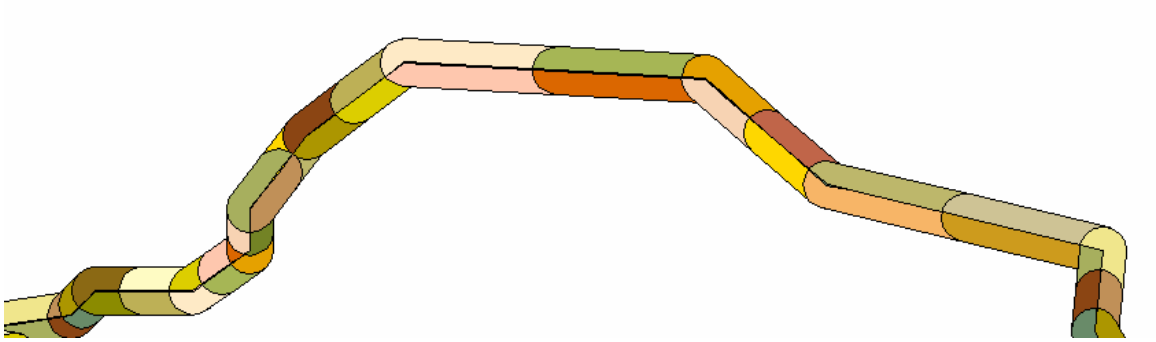

5) Differences in area between buffers on each side of a line segment were used to calculate the amount of bend in degrees in each segment. Angle was normalized by segment length for units of degrees per meter of stream length. Red areas in the image below show areas with greater potential for stream bank instability.

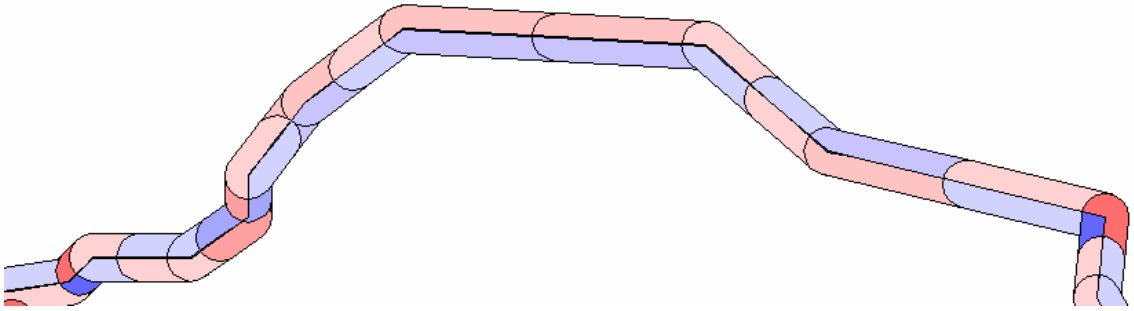

6) Finally the vector data were converted to a grid with the same resolution as the original DEM. The final map is shown in Figure 2.4.2.

7) Because of the generalization, there can be up to a 21 meter displacement between the generalized stream location and the flow accumulation stream. To reduce overlay errors we used only the absolute value of the curvature.

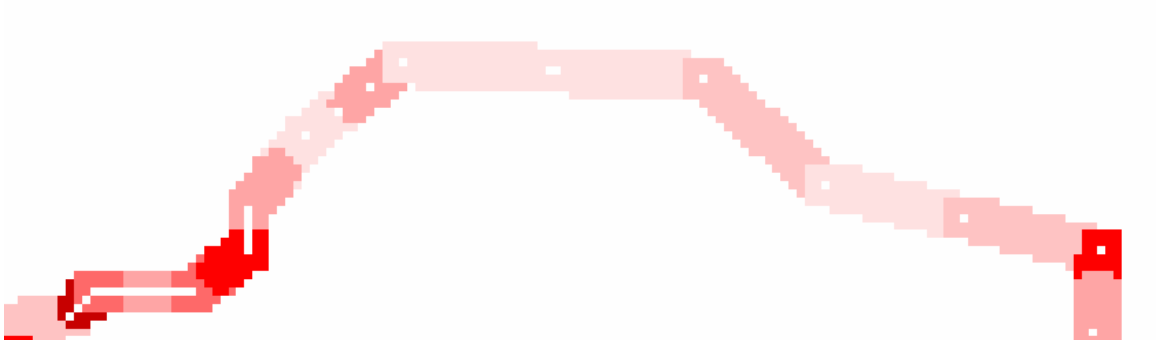

The method presented here was done without software development using freely available ArcView extensions and scripts, but has limitations in both scope and resolution. It required simplifying the original GIS data into straight segments, which resulted in the loss of data detail. Because this method relied on paired buffers, it did not work at stream intersections. The method resulted in many overlapping polygons. There were not suitable tools available in ArcView to properly resolve these overlapping areas into grids. Software packages, such as ArcGIS, can be extended via custom software to properly identify curvature in the original curvilinear GIS data. We recommend this approach for future projects.

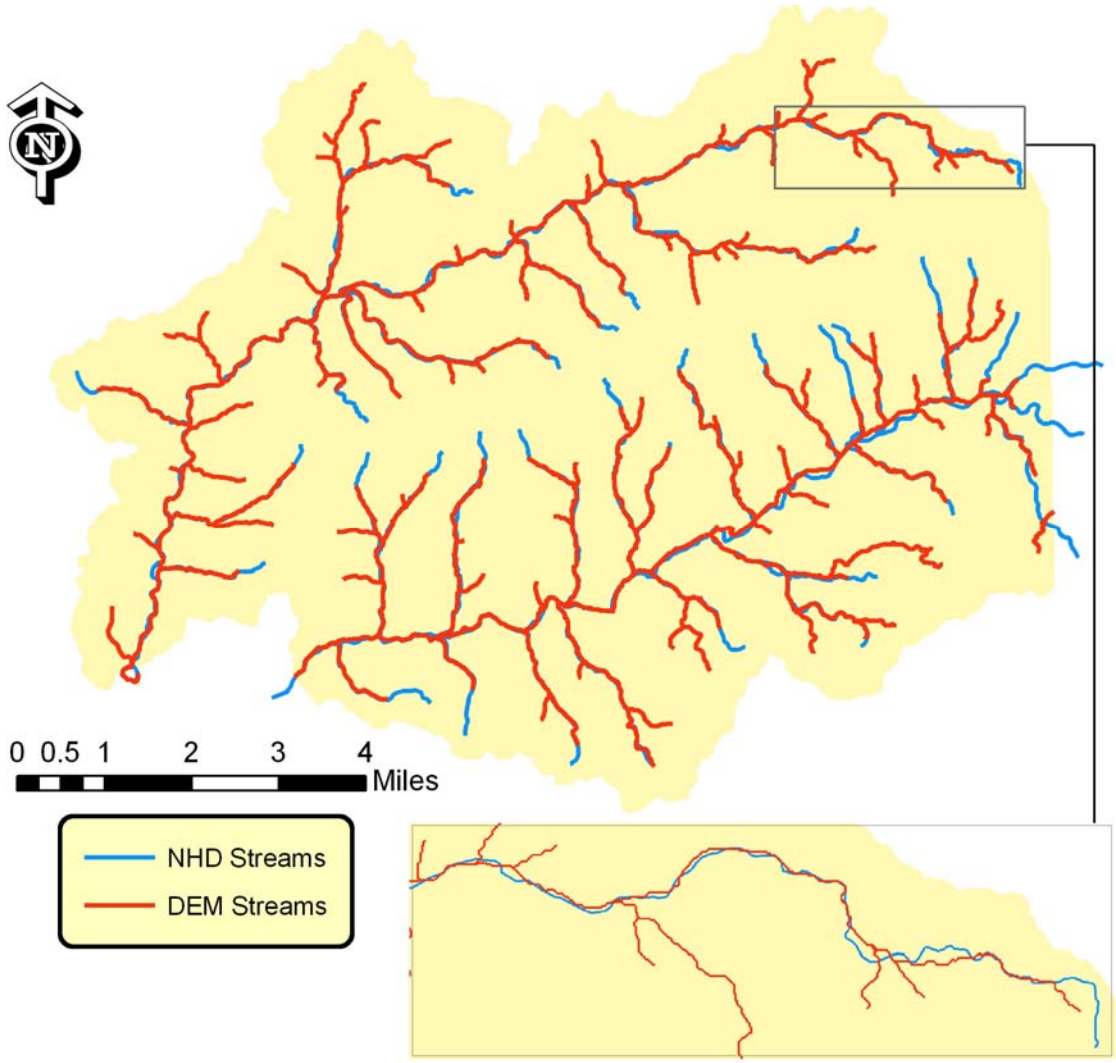

Figure 2.4.1 National Hydrography Dataset (NHD) and Digital Elevation Model (DEM) derived streams.

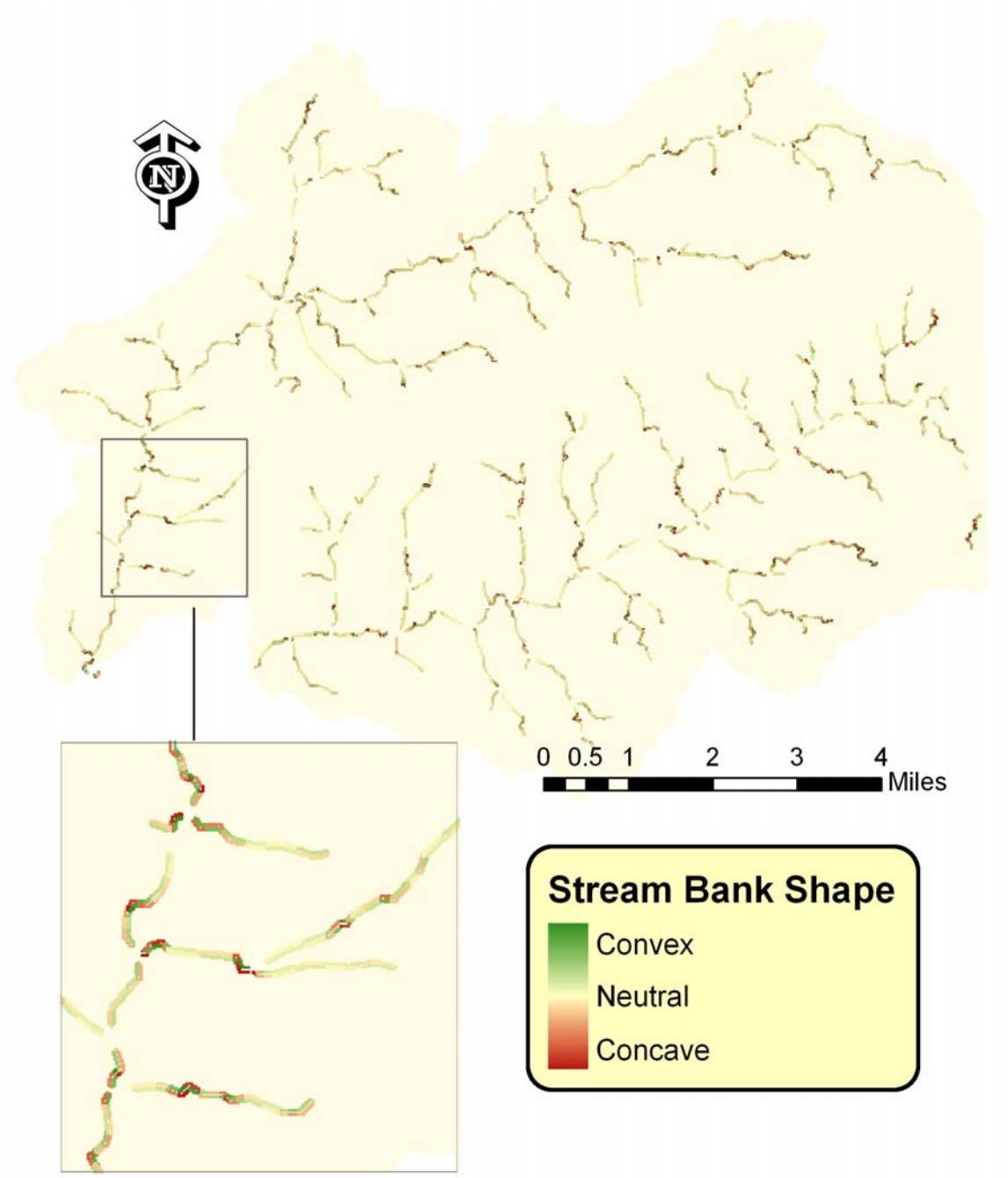

Figure 2.4.2 Curvature by stream segment within the study area. Higher stream bank erosion potential in concave sections (cut banks). Deposition likely in convex point bars.

(2.5) Stream Order and Gradient

Stream order is a simple method of stream classification based on the number of upstream tributaries. There are several methods of used to calculate stream order. We chose to use Strahler (1952). According to this method, a stream with no tributaries is a first order stream. The confluence of two first order streams forms a second order stream. A third order stream is formed by the confluence of two second order streams. Stream order increases in a downstream direction with drainage area. Stream characteristics are generally correlated with stream order in a given basin. Stream orders in the study area are given in Figure 2.5.1.

Stream gradient was estimated using the watershed delineation functions of the SWAT model (Figure 2.5.2). Stream gradient was highly correlated with stream order. Gradient deceased in a down stream direction with a typical concave line (Figure 2.5.3). Other stream characteristics such as drainage area, channel width and depth, flow velocity, bed grain size, stored sediment, and discharge were also correlated with stream order. These other characteristics were not measured in this study, but the general relationships are well documented (Stream Corridor Restoration: Principles, Processes, and Practices, (1998)). The general relationships are given in Figure 2.5.4.

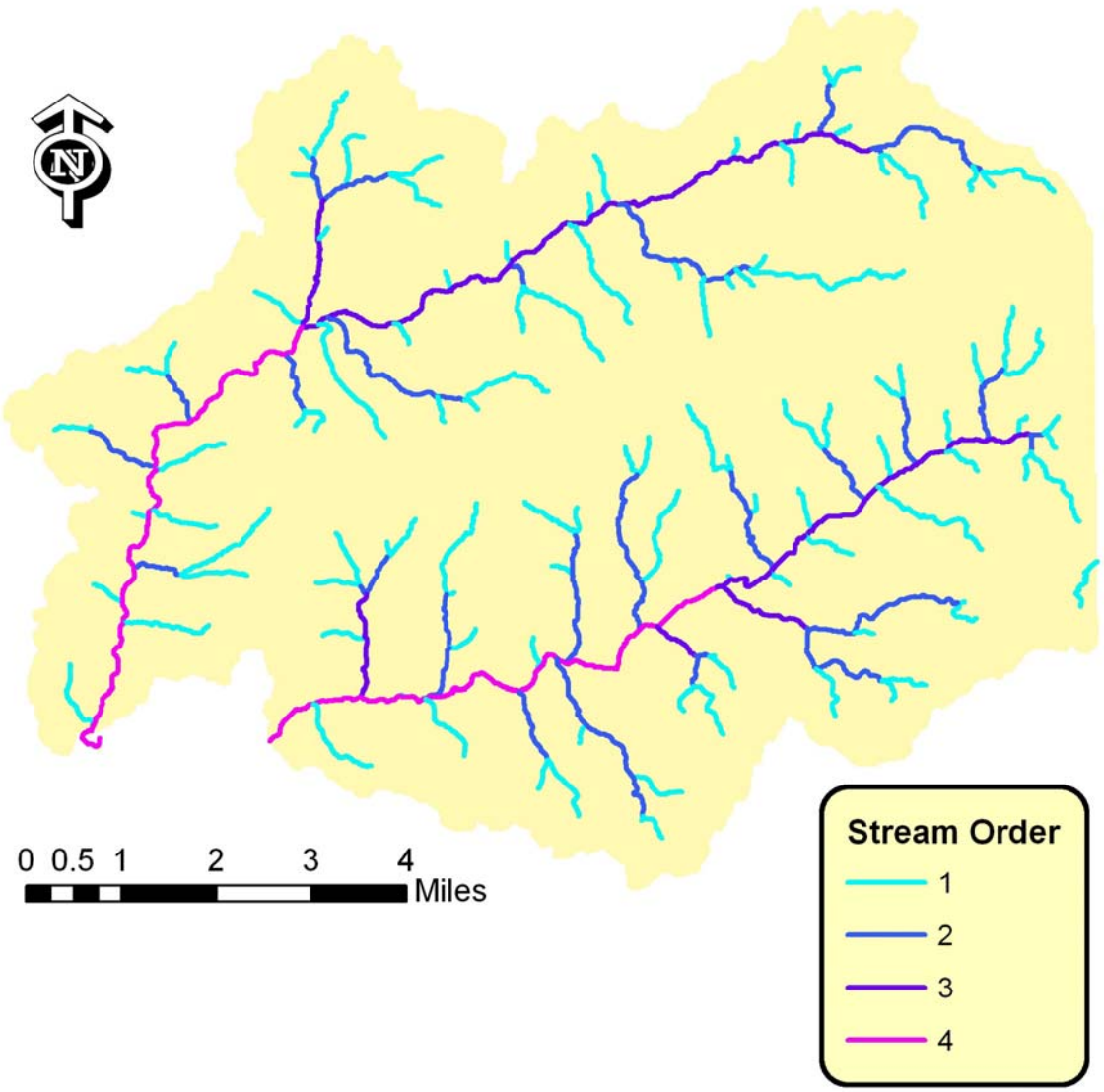

Figure 2.5.1 Straher (1952) stream order in the study area.

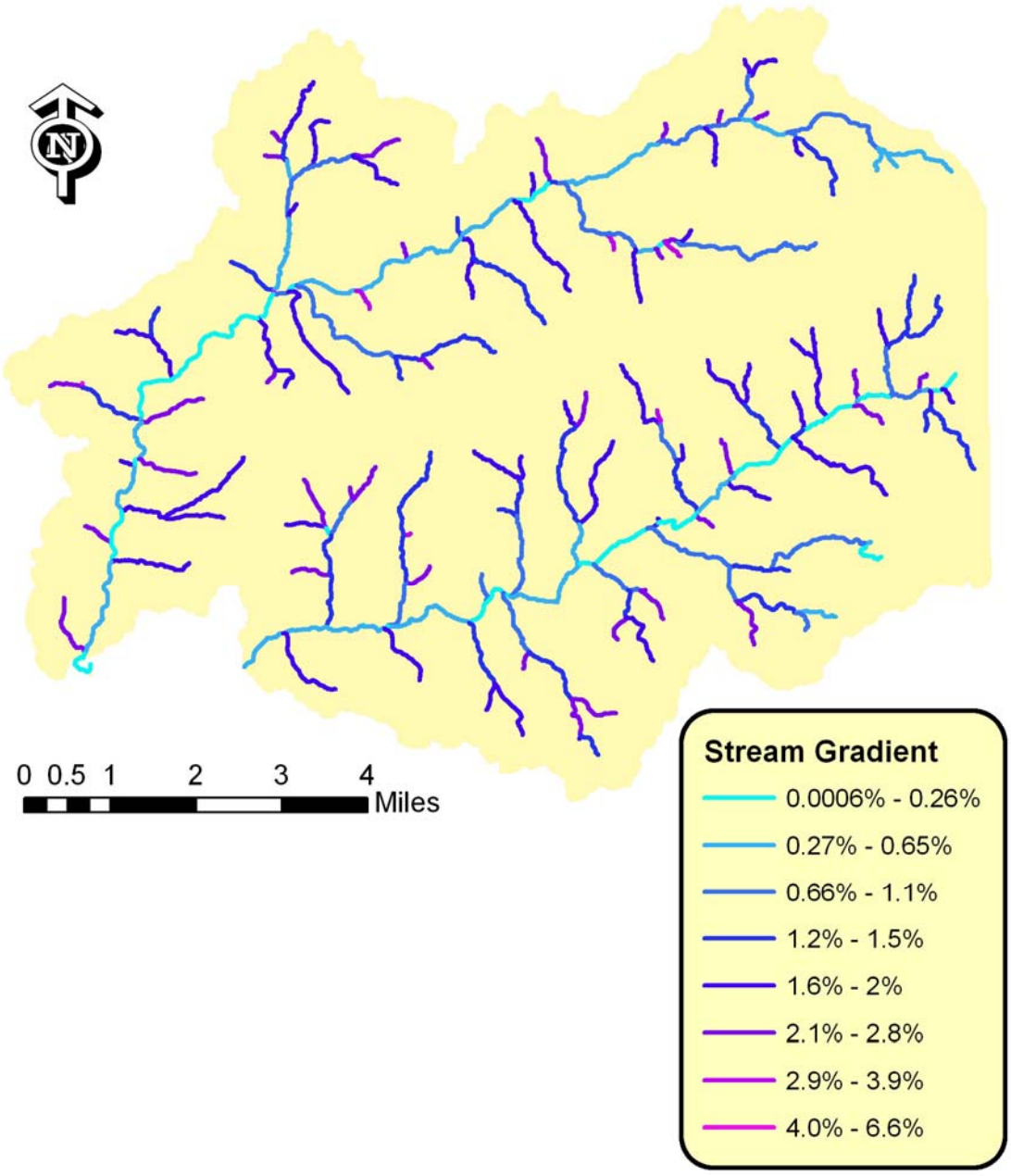

Figure 2.5.2 Soil and Water Assessment Tool (SWAT) estimated stream gradient in the study area.

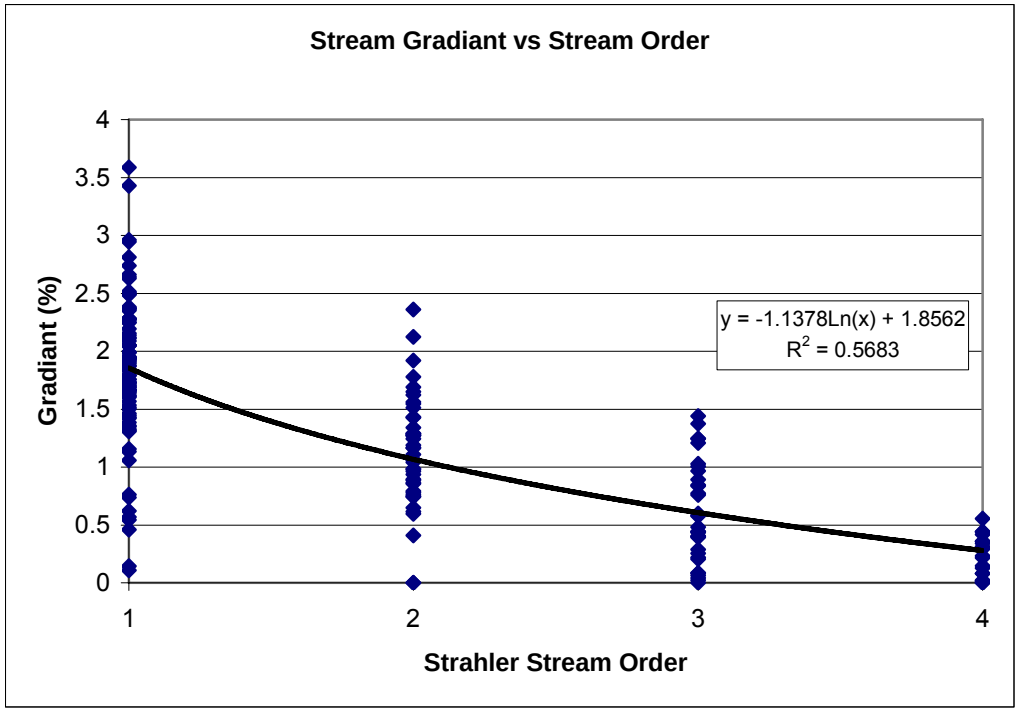

Figure 2.5.3 Relationship between stream order and stream gradient for segments longer than 200 meters within the study area.

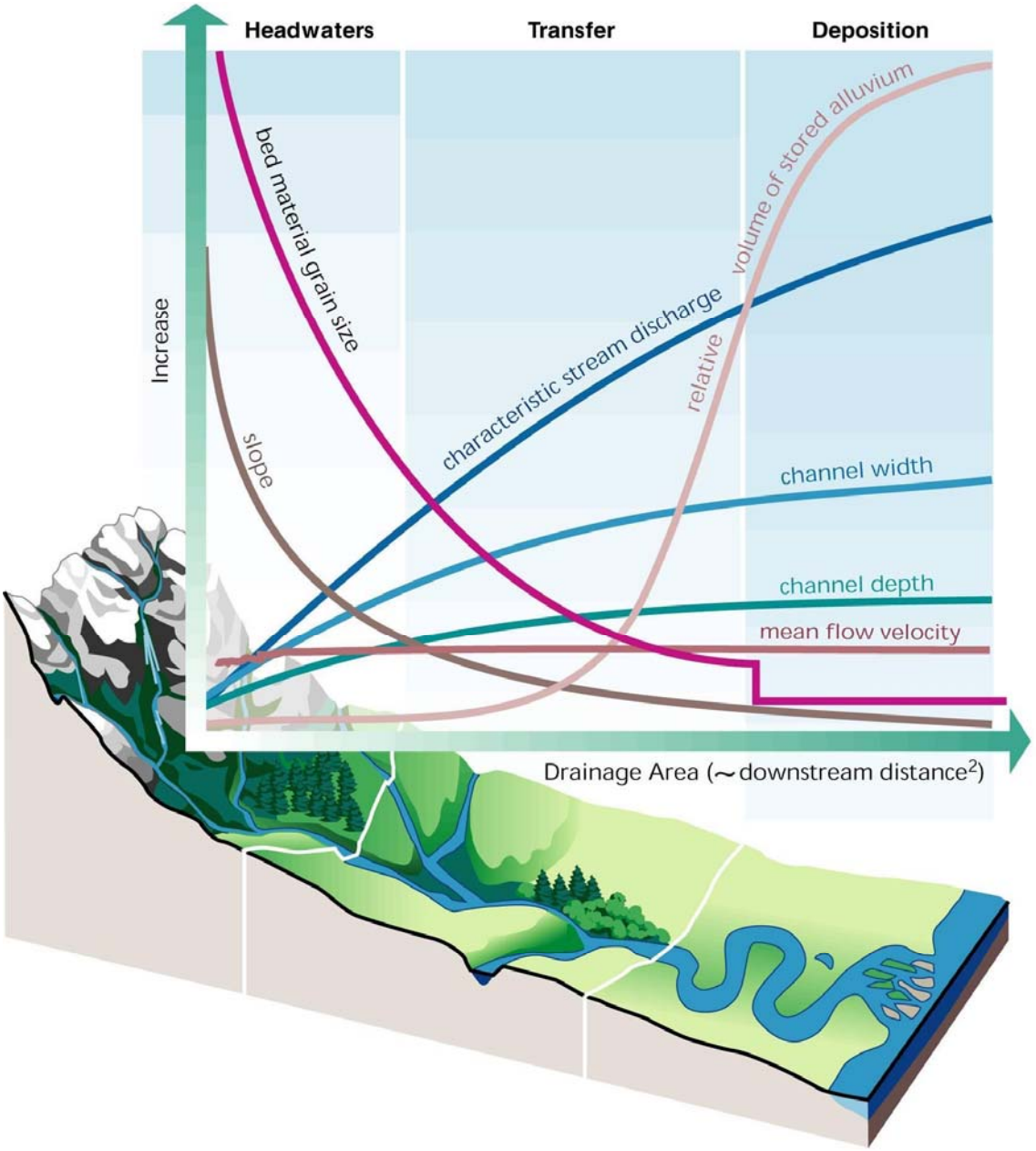

Figure 2.5.4 Generalized relationships by drainage area. Reproduced with permission (Stream Corridor Restoration: Principles, Processes, and Practices, (1998)).

(2.6) Riparian Targeting

Buffer and Mask development

Only a small fraction of the basin was considered for riparian targeting. We applied a buffer of 50 meters to each side of streams with a drainage area of at least 50 ha. It is unlikely that perennial streams would have a smaller drainage area unless spring fed, which is possible given the karst topography. Only areas within this 50 meter buffer were considered.

Additional areas within the buffer were excluded based on the runoff accumulation grid. Accumulations produce exceedingly high values in cells with channelized flow. This includes both the stream channel on which the 50 meter buffer was based and channelized flow from areas with drainage less that the 50 ha required to form a stream. Cells which contain channelized flow were not suitable for riparian buffers, which function with sheet flow only. Channelized flow short circuits the buffer, delivering the flow directly to the stream. The amount of runoff accumulation required to produce flow which was sufficiently channelized to short circuit riparian buffers was not clear. In future projects, this should be determined by field examination of sites with various levels of runoff accumulation. The focus of this project was to explore and define methodology, which can be refined with field data when applied. For this reason a runoff accumulation cutoff of 1000 was selected based on visual inspection of the GIS data and professional judgment. Because the runoff accumulation grid was normalized to an average value of 1 before the accumulation, a value of 1000 is roughly equal to the runoff produced from 1000 average cells or about 10 ha. The actual area will be larger in low runoff producing areas such as forest and smaller in higher runoff producing areas. The final buffer which was used to mask all data layers is given in Figure 2.6.1.

To perform targeting, we must consider whether the goal was restoration of degraded riparian zones or protection of existing forested ones. Both can be done using the same data by examining the current landcover in conjunction with the factors detailed in previous sections. Landcover was reclassified into a boolean grid based on the quality of the existing landcover with respect to riparian buffers, for use as a mask. Landcovers having a positive benefit in riparian zones were reclassified as true, all others were considered false. The reclassification scheme is shown in Table 2.6.1 and mapped in Figure 2.6.2. These data were used to assess the current state of riparian zones within the area of study.

Targeting

The final targeting maps were a compilation many factors. Each of the following factors is an indicator of riparian effectiveness or characteristics:

1. Landcover within riparian zone (Boolean) (LC)
2. Erosion predicted in riparian zone (ER)

3. Erosion accumulation from adjacent areas (EA)
4. Runoff accumulation from adjacent areas (RA)
5. Soluble phosphorus accumulation from adjacent areas (PA)
6. Stream curvature (SC)
7. Stream order (categorical)
8. Drainage area (DA)
9. Stream gradient (SG)
10. Buffer slope (BS)

The final targeting map was calculated as:

$$TI = LC\ (W_{ER}*ER + W_{EA}*EA + W_{RA}*RA + W_{PA}*PA + W_{SC}*SC + W_{DA}*DA + W_{SG}*SG + W_{BS}*BS)$$

where TI is the targeting index, W_X is the respective weighting factor for factor X, and factor abbreviations were defined in the list above.

Because these data had different means and distributions, factors were not directly comparable. Without comparable factors it was very difficult to define appropriate weights. To make these factors more comparable, each was transformed and normalized. No single parametric transformation could be applied to all factors to generate similar distributions. Similar distributions were required to make factors directly comparable. Nonparametric statistical tests avoid assumptions of data distribution by ranking data; a similar approach was applied here. After clipping each parameter grid to the 50 meter buffer mask, these data were broken into 20 quantiles using Arcview. Each quantile had roughly the same number of cells, 5% of the buffer area. The 20 quantiles were reclassified from 0 to 1 in 0.05 increments; the 0.95-1 quantile contained the highest valued original parameter cells. The resulting range was defined from 0-1 and the distribution was uniform with a mean of 0.5. The transformed and normalized data are given in Figures 2.6.3 to 2.6.10.

Weighting factors determined the relative importance of each factor in the final targeting map. Some data such as stream order were categorical and could not be directly used in the targeting. However, stream order is highly corrected with the drainage area factor and thus was indirectly accounted for in the final targeting. How each factor contributes to the effectiveness of a proposed or existing forested riparian buffer cannot be easily quantified. Without additional data the weighting factors can only be subjective estimated, based on professional judgment and a general understanding of how riparian buffers function. Each factor was selected and calculated to be an indicator of riparian functionality, however some factors were likely to be more important that others. Several factors were correlated with other factors, indicating that both contain at least in part, the same information. Correlation between factors must be considered when setting weighting factors. Correlation between factor grids is given in Table 2.6.2. As expected, factors based on flow accumulation are highly correlated (>0.81). The curvature factor was poorly correlated with any other factor, indicating that the information it contains is unique among all factors.

The intended benefit of the riparian buffer must also be considered. There are many pollutants, such as nitrogen, phosphorus, pesticides, metals, and sediment, which are controlled to varying degrees by riparian buffers. Riparian buffers also impact stream temperature, woody debris content, and wildlife populations. Although these were not considered in this research, other factors could be included based on landscape metrics, such as connectivity and diversity, which were correlated with habitat quality.

To better grasp the importance of each factor, field data are needed. Site visits could verify the utility of flow accumulation based factors. Although the removal of nutrients cannot be directly observed without expensive and elaborate field studies, areas of sediment deposition, stream bank instability, and channelization are visible. Although not quantitative, these data are still useful. Other data such as stream gradient and buffer slope can be easily verified. Unfortunately, field data were not collected in the study area to verify factors or to provide guidance determining factor weights. For this reason factor weights were not estimated, and assumed to be uniform.

Targeting maps were developed assuming all weighing factors to be 1.0 with the exception of buffer slope which was assumed to be -1.0. Buffer slope was known to have an inverse impact on trapping efficiency. Degraded riparian areas wee targeted and presented in Figure 2.6.10. Intact riparian buffers which were targeted for preservation are given in Figure 2.6.11.

Classification

Methods developed for remote sensing applications were adapted for use with these data. Image classification is the classification of an image consisting of several bands of correlated information. Each band is a measurement of the reflected radiant energy within a narrow band of frequencies. A natural color image is comprised of three bands: red, green, and blue. Image classifiers seek to identify surface features based on patterns within these bands. This pattern is the spectral signature. Many features, such as a particular landcover, have unique spectral signatures that can be used to identify all pixels of that landcover within an entire image. Signatures are developed by examining pixels at several locations within an image known to be the feature of interest. Our factors can be thought of as bands. If field surveys of the study area could determine several examples of highly effective riparian buffers, we can locate similar areas for restoration or preservation by developing the signature of an efficient buffer in the available factors, and locating that pattern elsewhere in the study area.

Signature development requires knowledge of existing features or in this case riparian effectiveness. Although we did not have ground truth data characterizing riparian buffers, the factor grids were calculated as indicators of riparian effectiveness. There were methods to classify data without predefined signatures called unsupervised classifiers. These methods identify groups of

pixels with similar characteristics, without any knowledge of exactly what features each group represents. One such method called isoclustering, or iterative optimization clustering procedure, was used to define categories within the study area with similar riparian characteristics as defined by our factors. ArcMap had an isoclustering component, but we were unable to include more than three bands using this software. To simplify these data into three bands, principal components analysis was used. Principle components analysis is a procedure to reduce the number of bands or dimensions of a dataset to facilitate further analysis while preserving the information present within the original data. Eight factors were reduced to three bands, shown in Figure 2.6.12. In this figure, bands were shown in primary colors; areas with similar factors had similar colors. These three bands were processed using isodata clustering to generate 30 categories (Figure 2.6.13). The mean factor values for each class are given in Table 2.6.3. Ideally ground truth would be used to identify which categories best identify riparian buffer suitability.

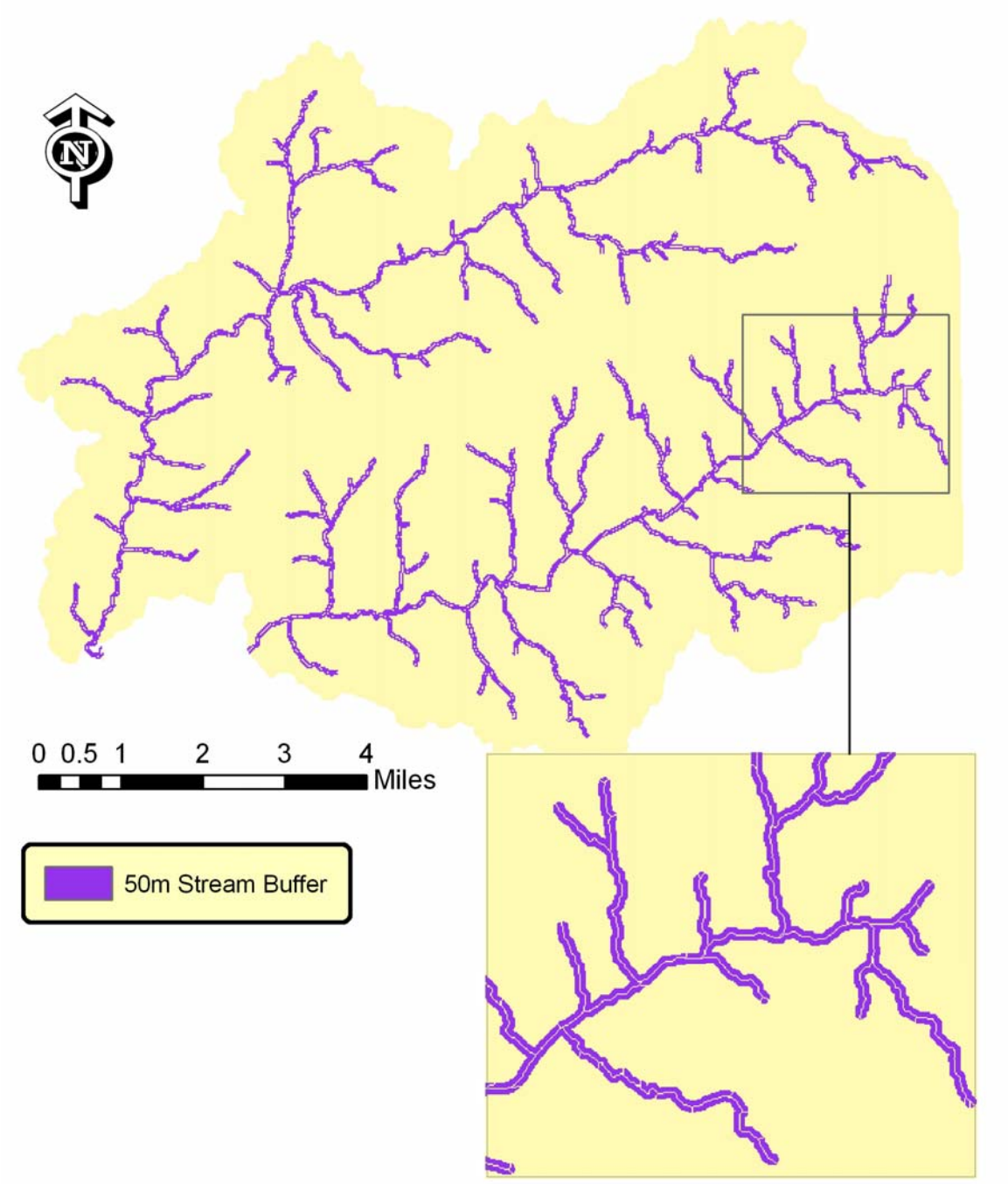

Figure 2.6.1 Fifty meter stream buffer for streams within the study area. Cells with highly concentrated flow were removed from the buffer area.

Table 2.6.1 Landcover reclassification for riparian quality.

Landcover	Riparian Boolean Grid
High Biomass Pasture	False
Low Biomass Pasture	False
Brushy Rangeland	True
Urban	False
Wheat/beans	False
Forest	True
Bare	False
Water	True
Stream	True

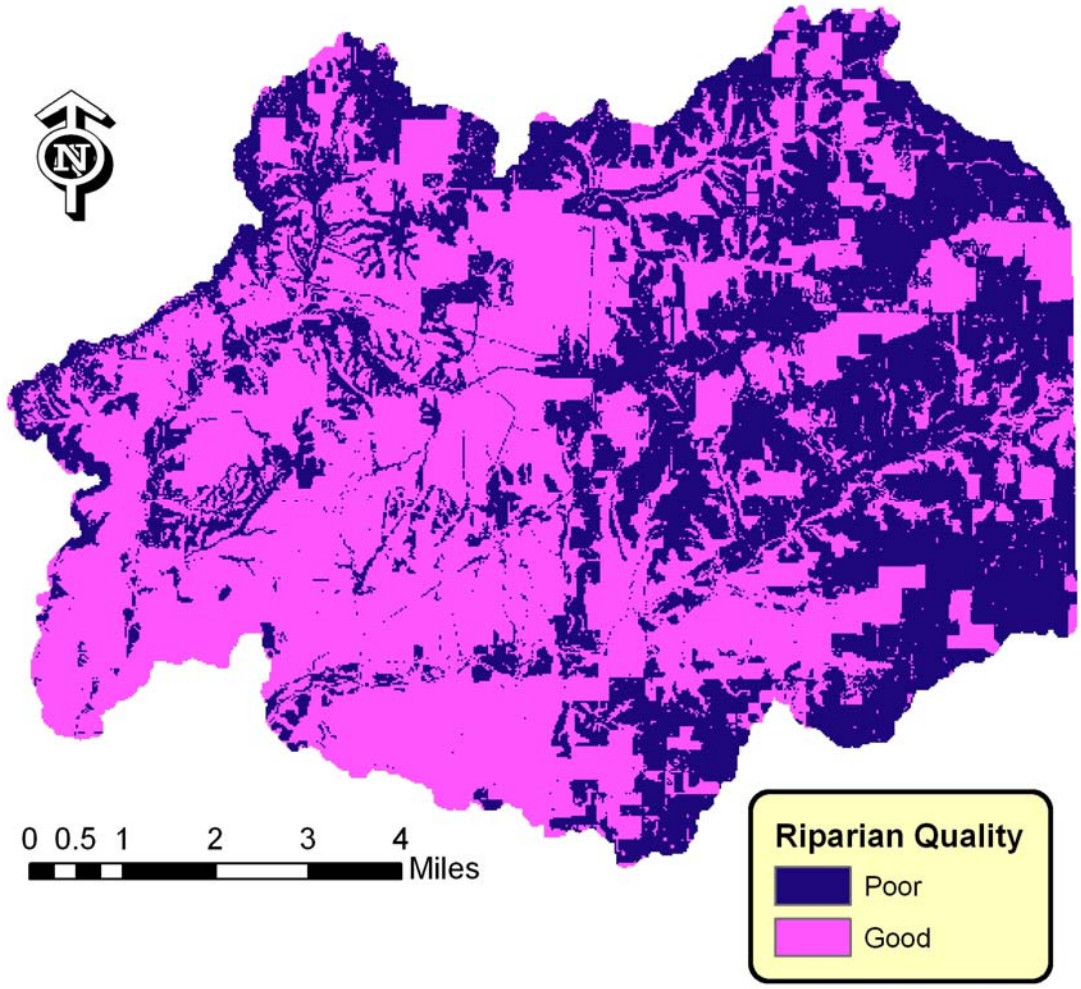

Figure 2.6.2 Landcover reclassified using Table 2.6.1. Good indicates landcovers such as forest, which are desirable in riparian zones.

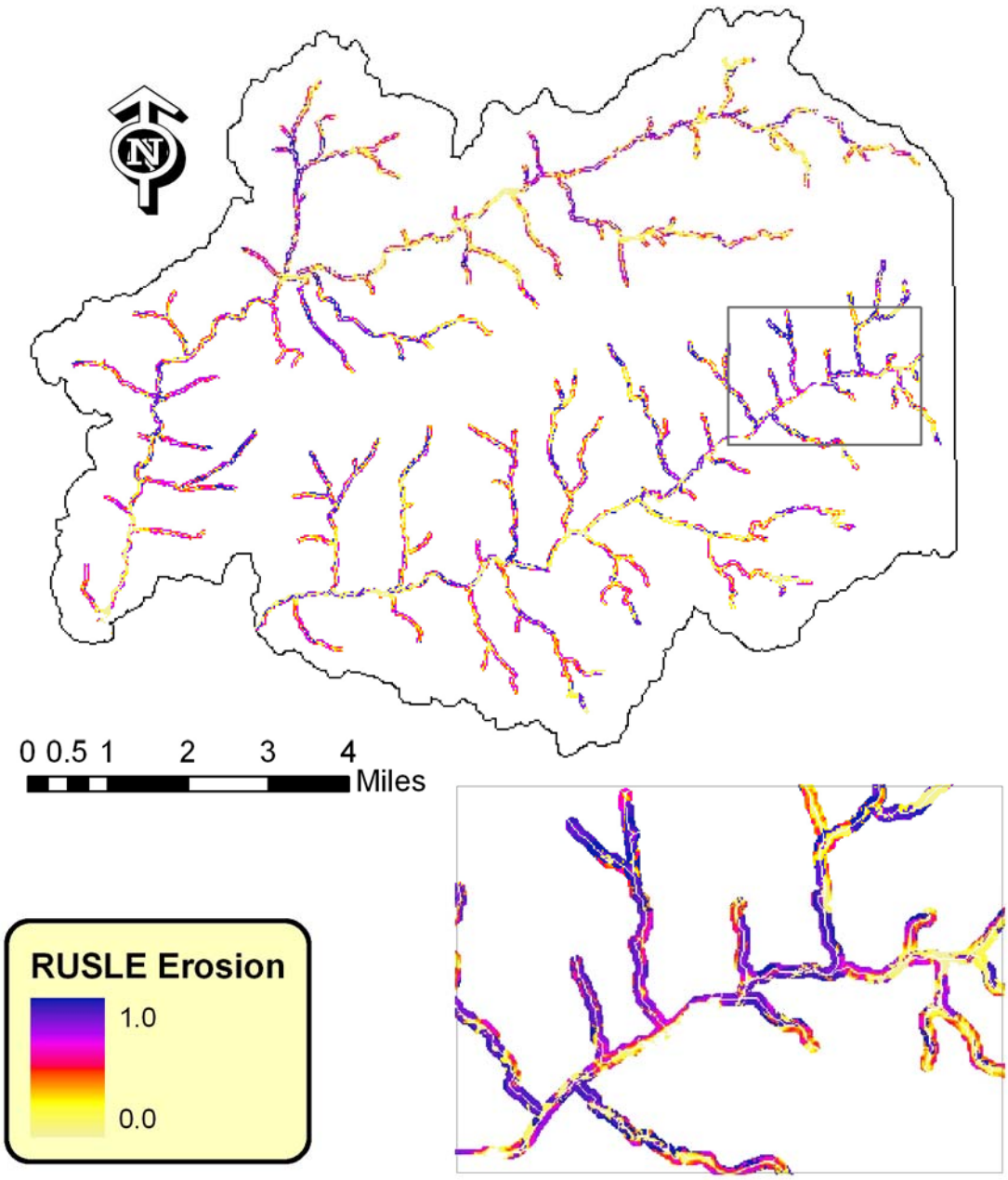

Figure 2.6.3 Normalized RUSLE erosion based index for the study area within a 50 meter stream buffer.

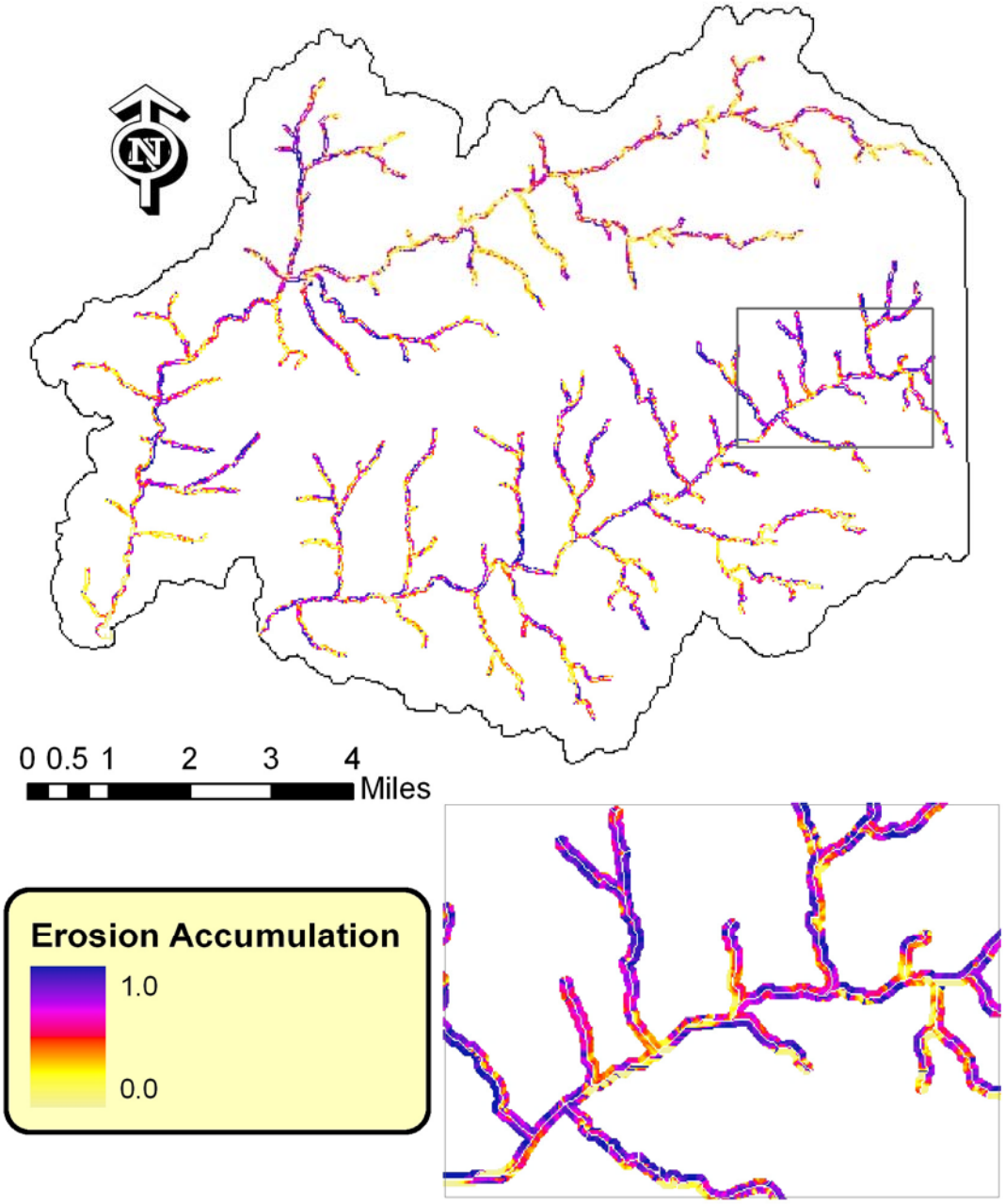

Figure 2.6.4 Normalized RUSLE erosion accumulation from adjacent areas index for the study area within a 50 meter stream buffer.

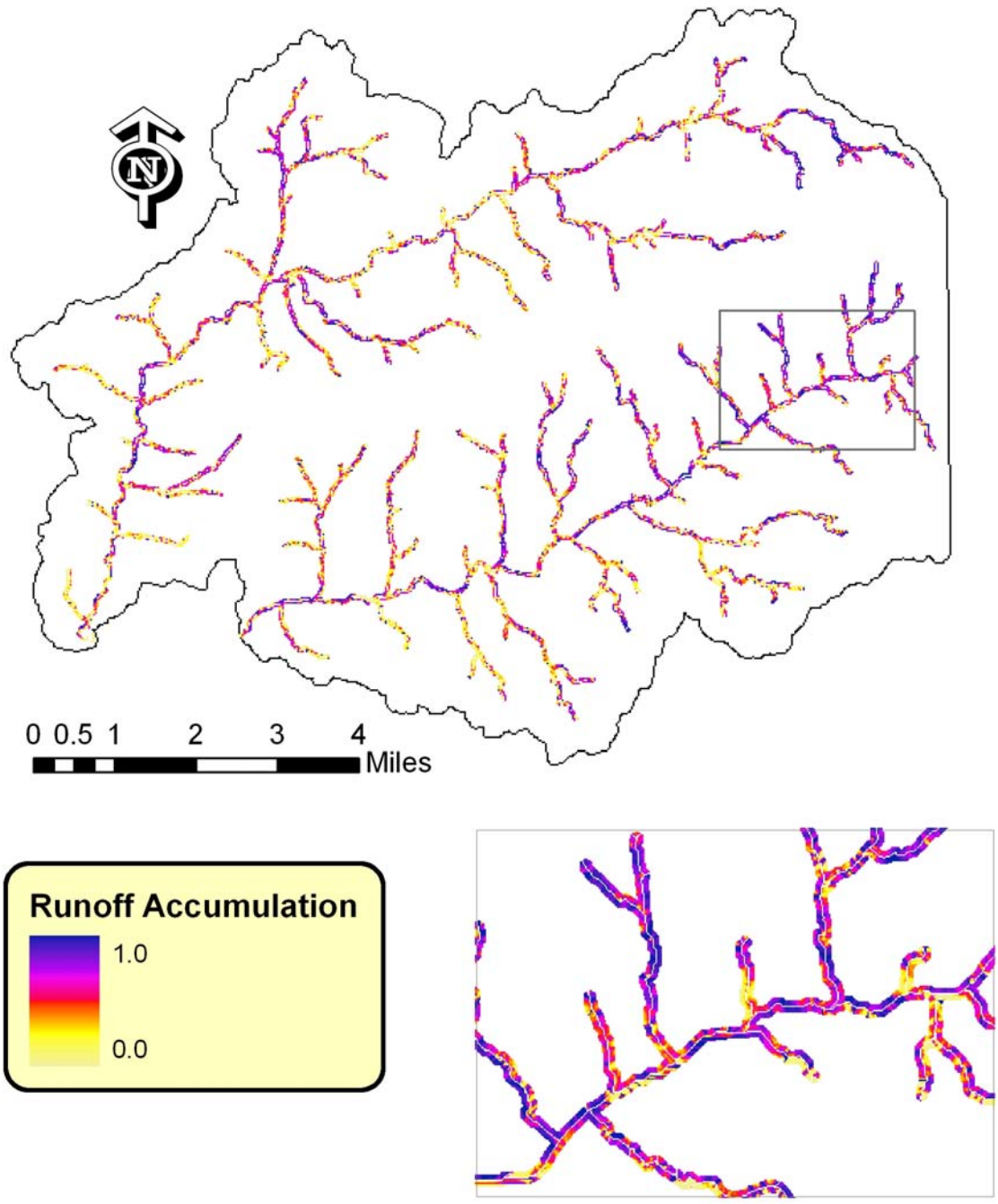

Figure 2.6.5 Normalized runoff accumulation from adjacent areas index for the study area within a 50 meter stream buffer.

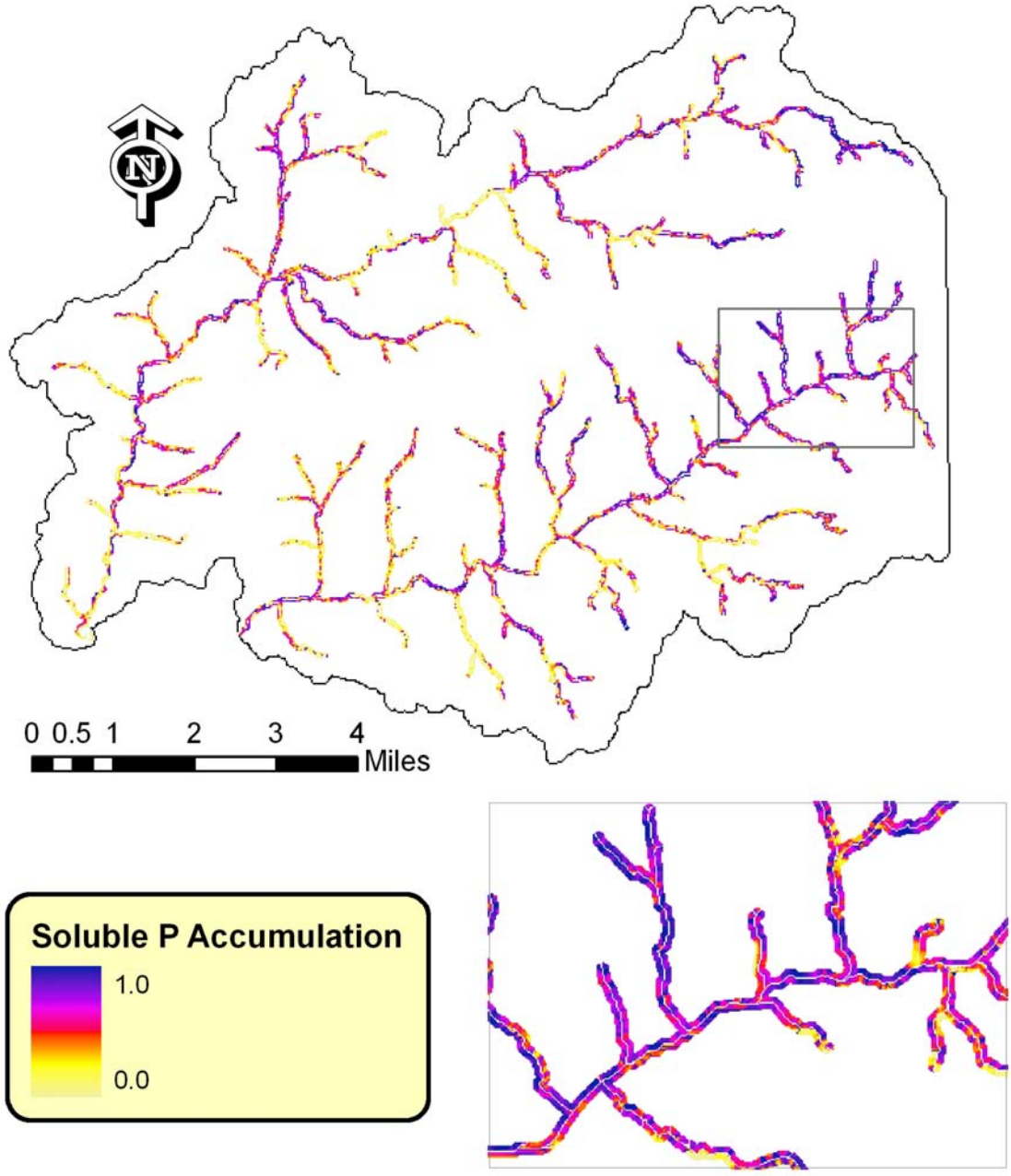

Figure 2.6.6 Normalized soluble phosphorus accumulation from adjacent areas index for the study area within a 50 meter stream buffer.

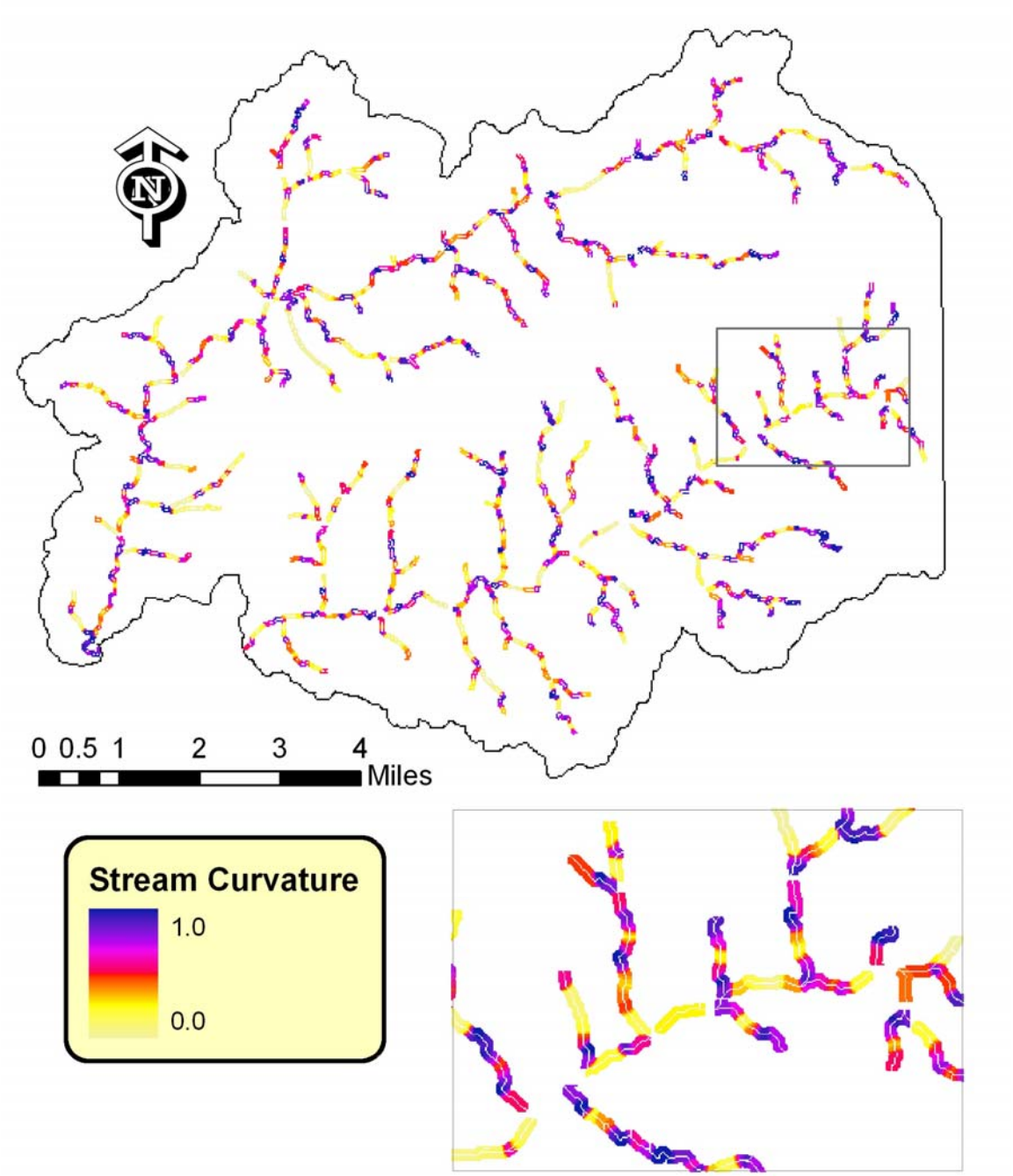

Figure 2.6.7 Normalized stream curvature based index for the study area within a 50 meter stream buffer.

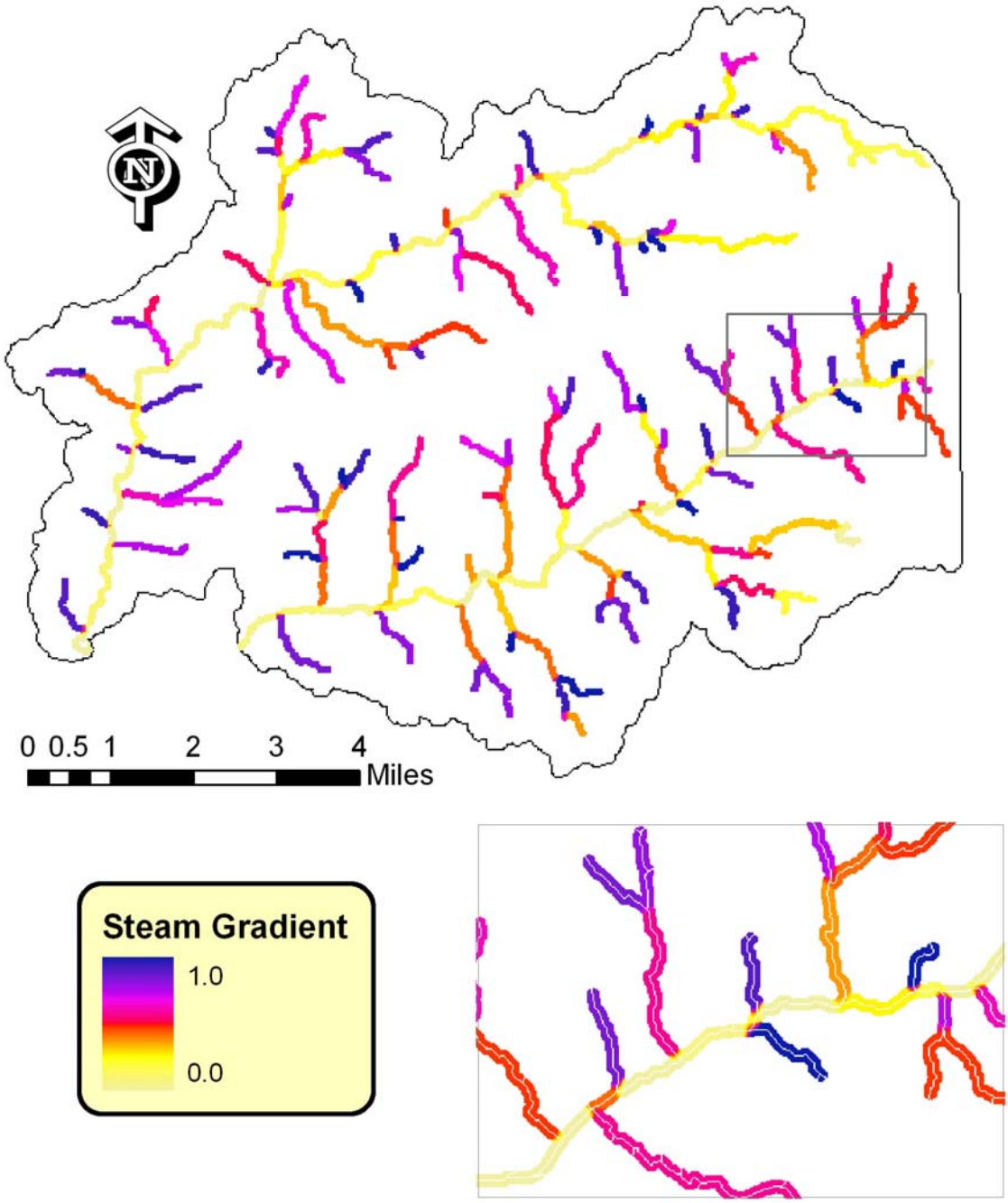

Figure 2.6.8 Normalized stream gradient based index for the study area within a 50 meter stream buffer.

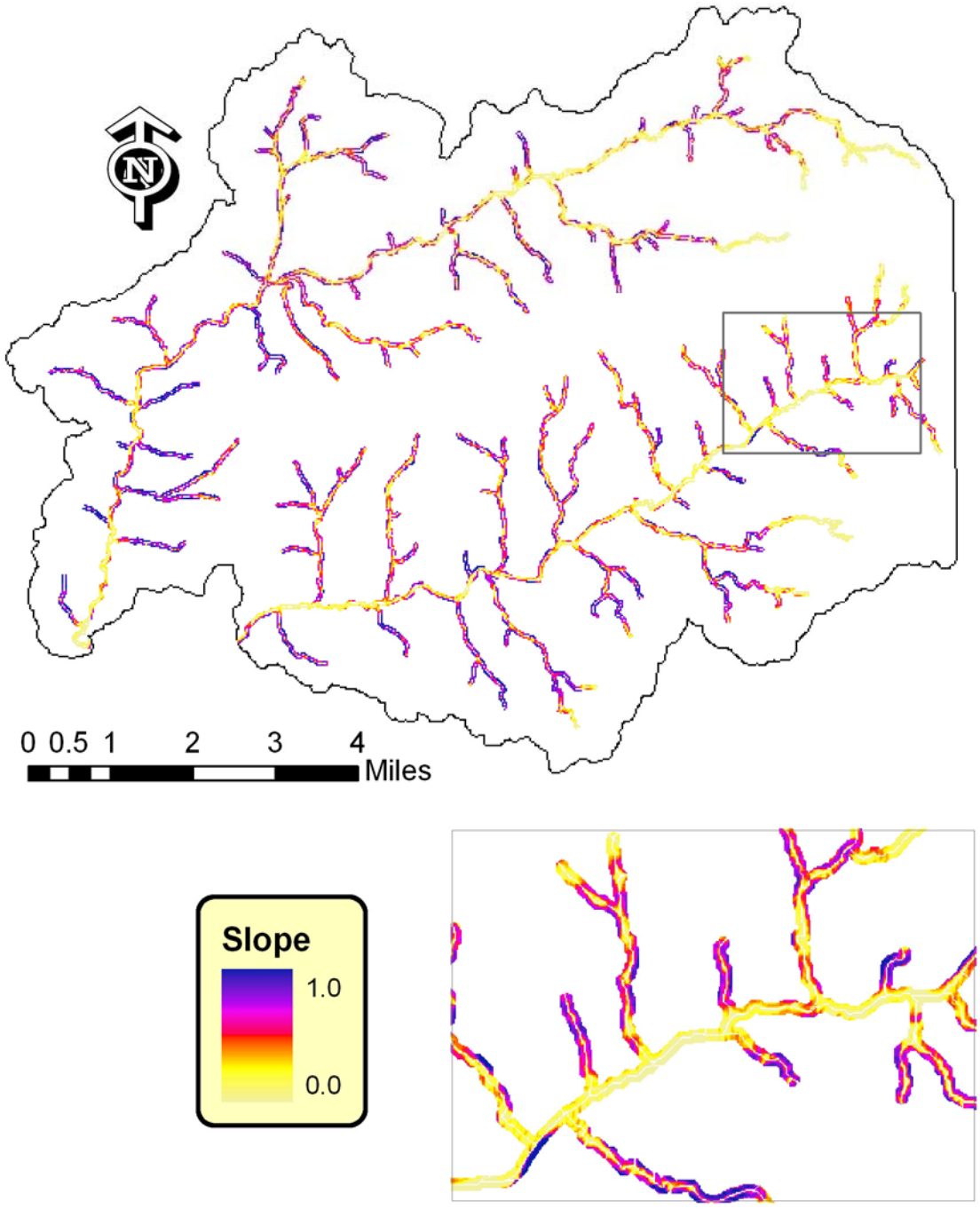

Figure 2.6.9 Normalized slope based index for the study area within a 50 meter stream buffer.

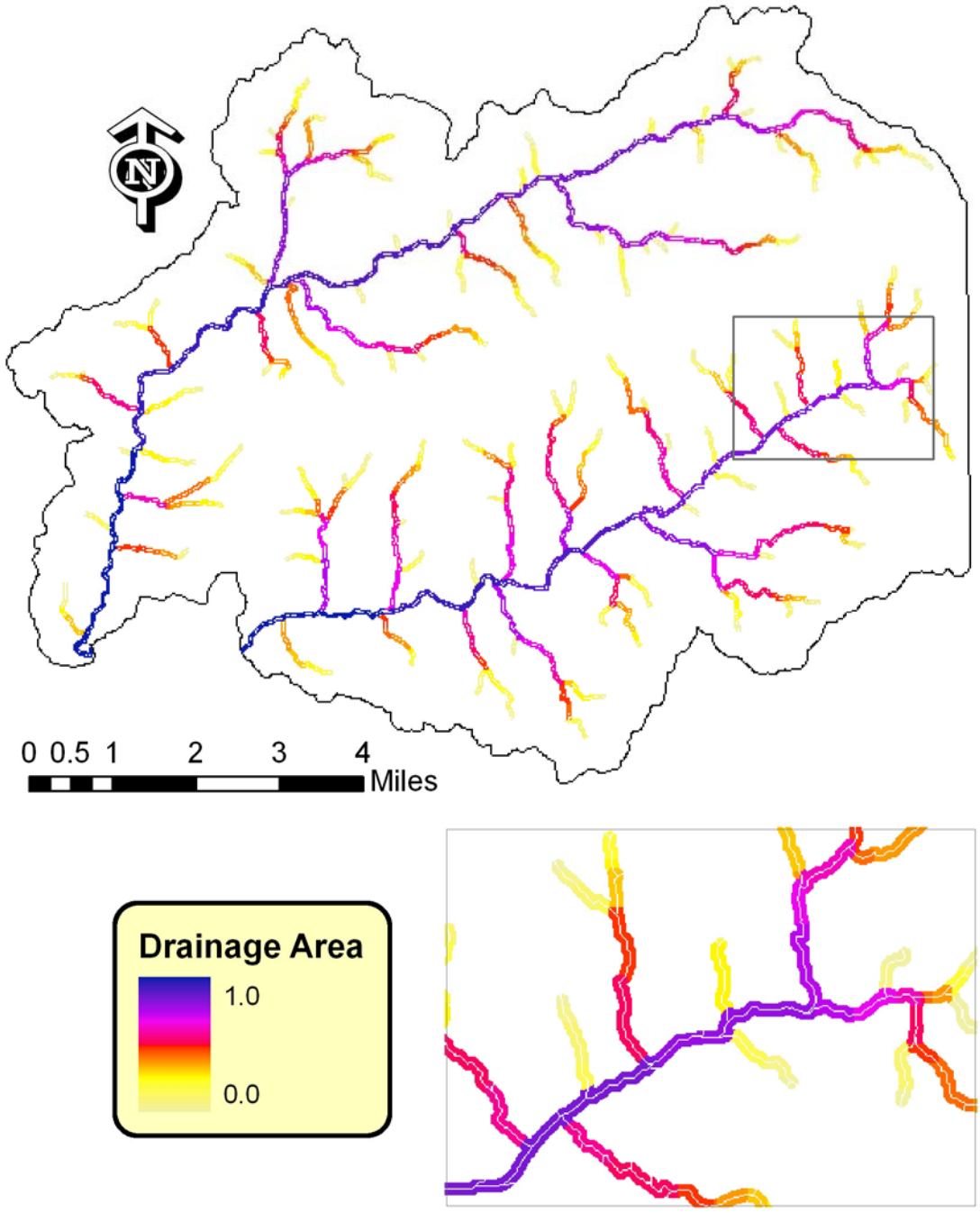

Figure 2.6.9 Normalized drainage area based index for the study area within a 50 meter stream buffer.

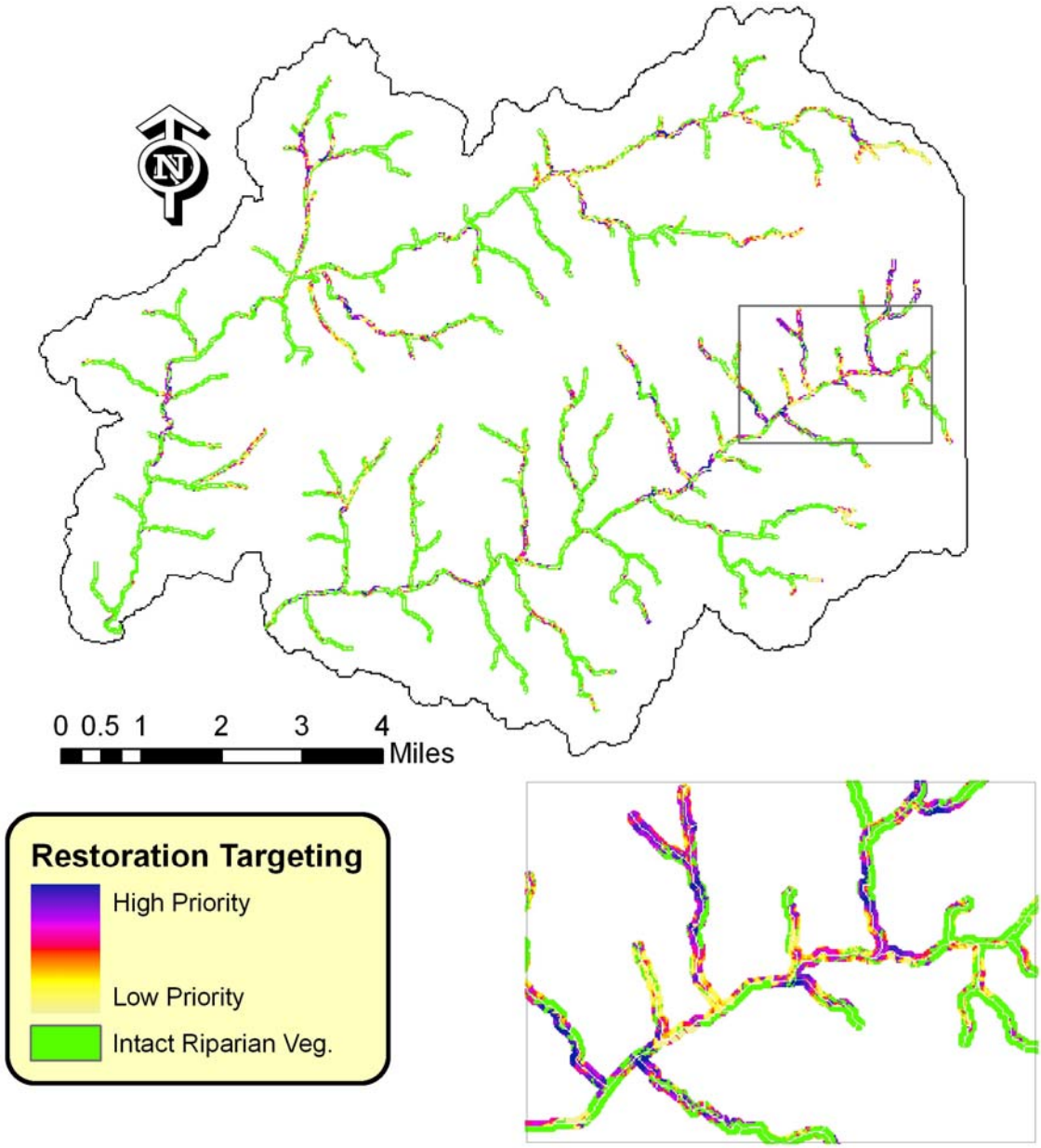

Figure 2.6.10 Targeting degraded riparian corridors, based on uniform factor weights.

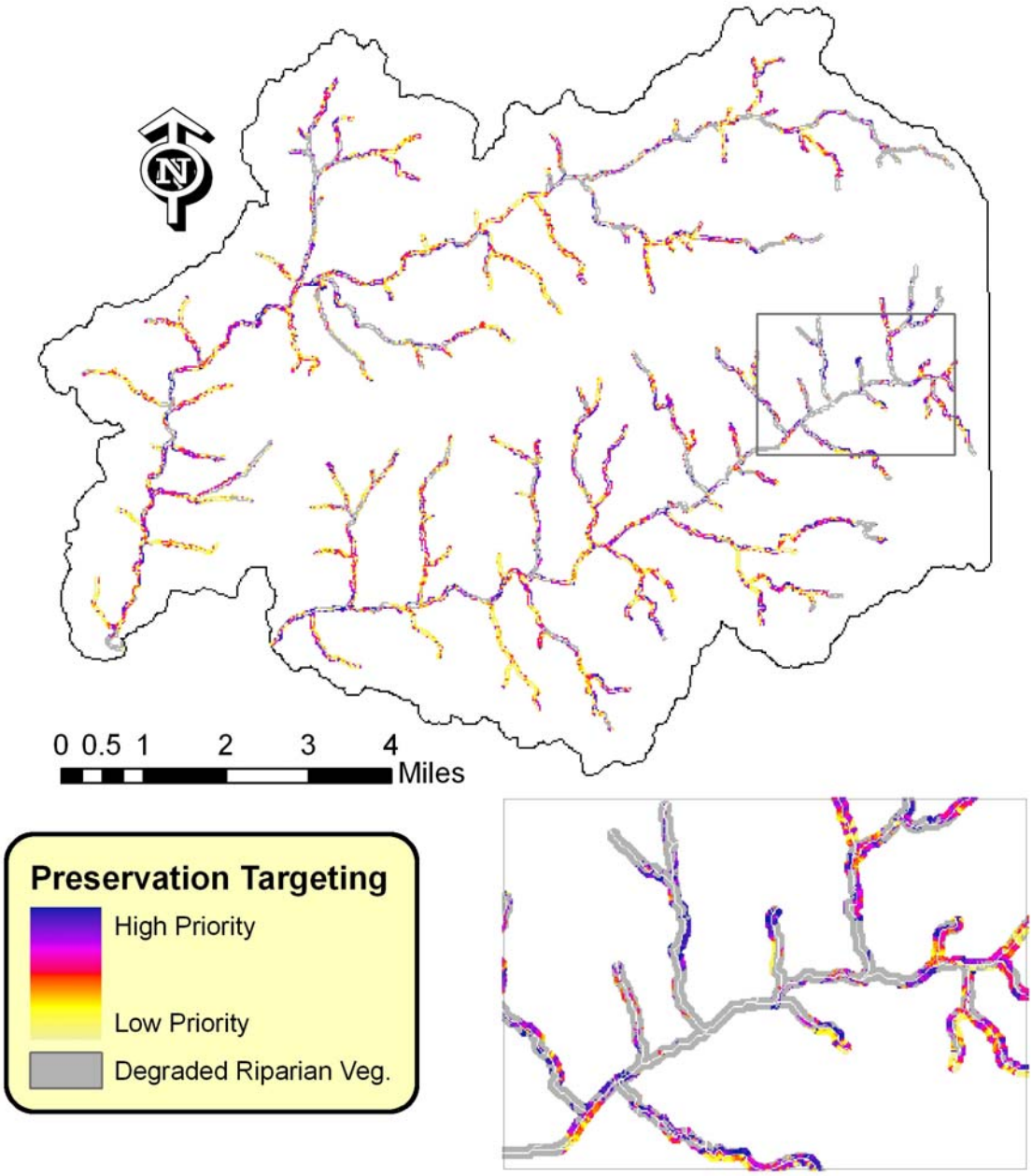

Figure 2.6.11 Targeting well vegetated riparian corridors for preservation, based on uniform factor weights.

Table 2.6.2 Correlation coefficient between factor grids in the study area.

Layer	Drainage Area	Curvature	Current Vegetation	Runoff Acc.	Stream Gradient	Buffer Slope	Soluble P Acc.	Erosion	Erosion Acc.
Drainage Area	1.00	0.06	-0.02	0.06	-0.75	-0.33	0.07	-0.08	0.06
Curvature	0.06	1.00	0.00	-0.06	-0.06	-0.13	-0.02	-0.09	-0.10
Current Vegetation	-0.02	0.00	1.00	-0.09	0.04	0.09	-0.13	-0.16	-0.08
Runoff Acc.	0.06	-0.06	-0.09	1.00	-0.15	-0.27	0.85	0.25	0.81
Stream Gradient	-0.75	-0.06	0.04	-0.15	1.00	0.47	-0.18	0.12	-0.04
Buffer Slope	-0.33	-0.13	0.09	-0.27	0.47	1.00	-0.35	0.34	-0.07
Soluble P Acc.	0.07	-0.02	-0.13	0.85	-0.18	-0.35	1.00	0.26	0.76
Erosion	-0.08	-0.09	-0.16	0.25	0.12	0.34	0.26	1.00	0.38
Erosion Acc.	0.06	-0.10	-0.08	0.81	-0.04	-0.07	0.76	0.38	1.00

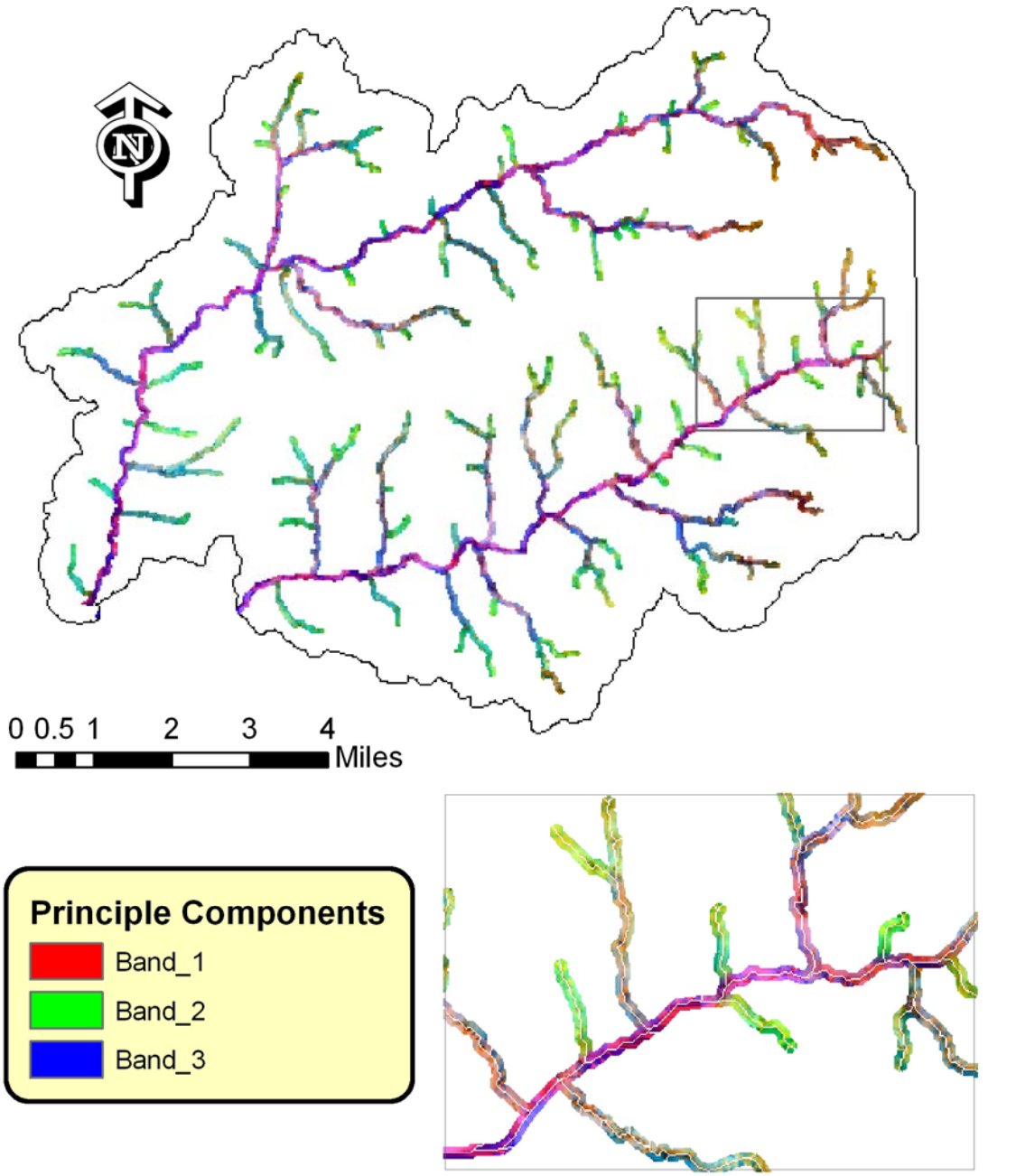

Figure 2.6.12 Principle components analysis of eight factors resulting in three bands. Similar colors represent similar factor values.

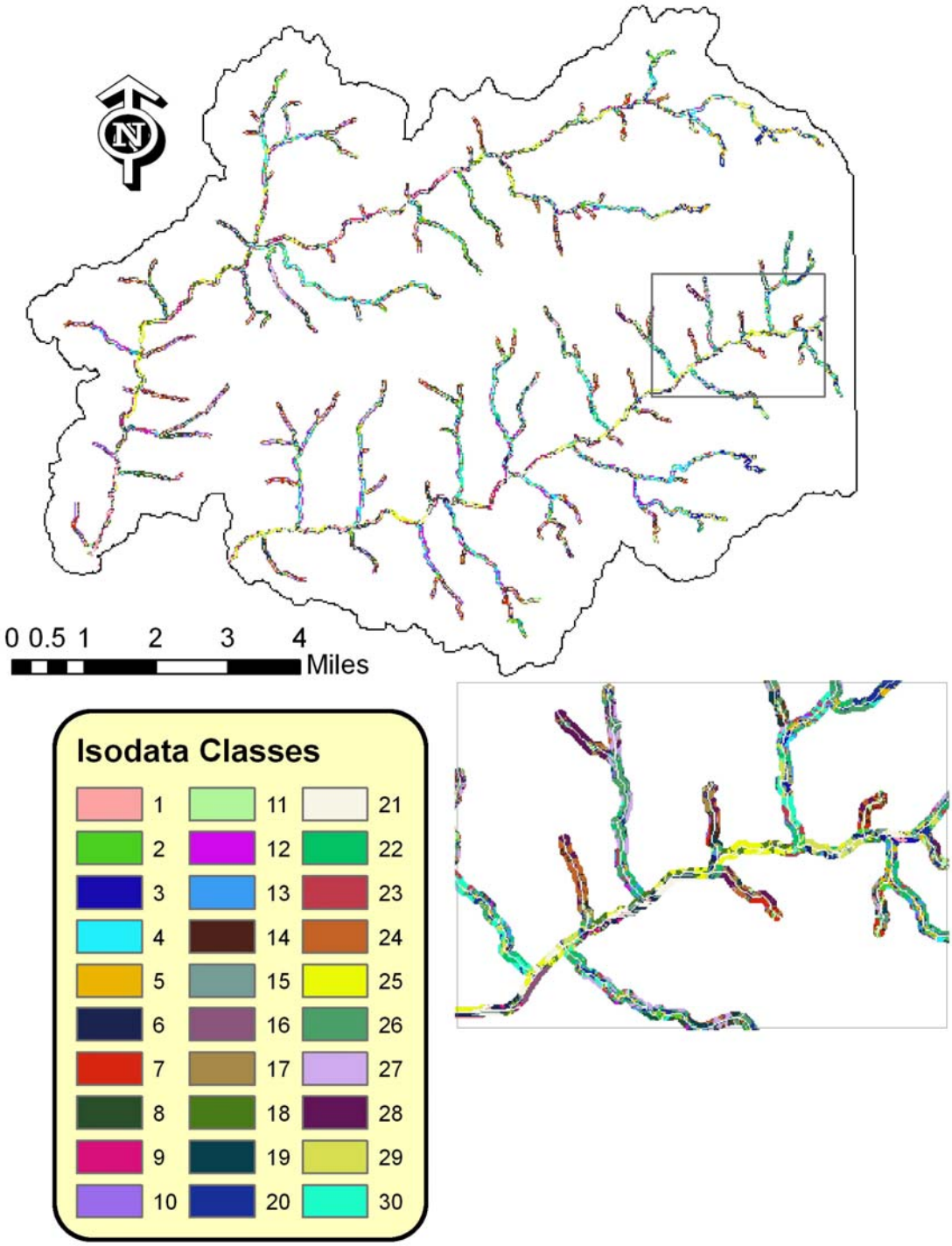

Figure 2.6.13 Isodata clustering results. Categories represent zones with similar characteristics as defined by factors.

Table 2.6.3 Isodata clustering classes for average factor value.

Isodata Class	Drainage Area	Erosion Acc.	Erosion	Soluble P Acc.	Stream Gradient	Runoff Acc.	Curvature	Buffer Slope	Total Indicator
1	0.91	0.08	0.08	0.15	0.17	0.10	0.64	0.81	2.93
2	0.38	0.17	0.15	0.22	0.67	0.18	0.69	0.61	3.08
3	0.57	0.15	0.12	0.36	0.34	0.21	0.77	0.83	3.34
4	0.64	0.17	0.29	0.16	0.45	0.17	0.54	0.37	2.79
5	0.44	0.36	0.19	0.51	0.45	0.51	0.66	0.75	3.87
6	0.87	0.32	0.20	0.41	0.19	0.36	0.59	0.76	3.70
7	0.22	0.19	0.33	0.18	0.83	0.17	0.56	0.29	2.77
8	0.42	0.20	0.48	0.13	0.67	0.16	0.49	0.13	2.68
9	0.89	0.27	0.41	0.26	0.18	0.26	0.48	0.39	3.13
10	0.21	0.23	0.58	0.14	0.87	0.18	0.36	0.05	2.63
11	0.24	0.44	0.26	0.45	0.78	0.45	0.62	0.52	3.76
12	0.63	0.35	0.62	0.24	0.46	0.30	0.42	0.11	3.12
13	0.62	0.47	0.46	0.43	0.46	0.46	0.52	0.46	3.88
14	0.23	0.44	0.58	0.36	0.82	0.38	0.43	0.14	3.38
15	0.80	0.54	0.19	0.62	0.23	0.64	0.59	0.79	4.40
16	0.91	0.50	0.71	0.41	0.14	0.40	0.45	0.25	3.76
17	0.19	0.69	0.43	0.69	0.82	0.70	0.58	0.42	4.53
18	0.89	0.59	0.63	0.62	0.15	0.59	0.49	0.62	4.58
19	0.32	0.59	0.59	0.51	0.71	0.52	0.48	0.28	4.00
20	0.34	0.70	0.20	0.86	0.49	0.87	0.64	0.78	4.87
21	0.89	0.81	0.18	0.86	0.14	0.87	0.53	0.84	5.13
22	0.59	0.67	0.59	0.70	0.46	0.70	0.55	0.56	4.81
23	0.67	0.73	0.84	0.60	0.41	0.59	0.39	0.31	4.55
24	0.22	0.72	0.80	0.58	0.83	0.57	0.37	0.16	4.26
25	0.90	0.83	0.80	0.85	0.15	0.84	0.44	0.62	5.42
26	0.37	0.87	0.63	0.89	0.61	0.90	0.57	0.59	5.43
27	0.38	0.87	0.87	0.78	0.67	0.79	0.32	0.34	5.01
28	0.17	0.88	0.75	0.88	0.85	0.87	0.49	0.36	5.24
29	0.69	0.85	0.52	0.93	0.31	0.93	0.59	0.76	5.58
30	0.68	0.91	0.87	0.87	0.40	0.88	0.41	0.50	5.53

(3) Principal Findings and Significance

The primary objective of this research was to develop a framework to best utilize existing data to predict the optimal placement of riparian buffers within a basin. This research incorporated both methods from previous studies, and new novel approaches to optimally place buffers. Several findings of this research are listed below:

- Currently available models lacked either the spatial detail or spatial extent to quantitatively target riparian buffers at the basin scale.
- Flow accumulation was a valuable tool to characterize water and nutrient movement over the land surface and through riparian buffers.
- Simple models like the RUSLE can be used to easily estimate gridcell erosion at a basin scale.
- Extrapolation of load or runoff by landcover and soil can produce adequate gridcell level estimates for an entire basin.
- Stream curvature may be a valuable predictor of current stream bank instability and future stream migration. Buffer distance may need to be increased in these areas to allow for future stream movement.
- Ground truth data are essential to develop appropriate weighting factors, and will be required in future applications of these methods.
- Principles adapted from remotes sensing can utilize examples of high priority riparian buffer to find areas with similar characteristics in an entire basin.

(3.1) Utility of Models

Process based models can predict the optimal placement of riparian buffers within a small watershed. Even these small models are very complex and difficult to parameterize. Available models and or combinations of models lack either the spatial extent (field scale models) or the process detail (basin scale models) to simulate hundreds or thousands of possible riparian buffers within a basin. Even though we have a reasonable understanding of the processes governing the movement of water and nutrients across the land surface and through a riparian buffer, we lack the computational power and data with which to parameterize a model with a large spatial extent. Currently available basin scale models aggregate input GIS data to reduce complexity. Lost are the subtle yet important details of aspect and slope which determine how water moves across the land surface to the stream. Gridcell versions of basin scale models may recapture this information at the expense of tremendous computational requirements. For these reasons we decided to use simple GIS based models with no aggregation of input data.

(3.2) Quantitative Limitations

The method as detailed in this study is qualitative in nature. This is an important limitation, and the consequence of using GIS indicators in lieu of process based models. Each factor proposed is an indicator of riparian buffer functionality, but the exact relationship is unknown. EPA and the 319 program are under pressure from Congress to estimate water quality improvements to justify allocated funds. Watershed models are quantitative by nature and will provide a number with varying degrees of uncertainty. Simplification and aggregation of input data increase this uncertainty as field scale processes are ignored or consolidated to accommodate limited computational resources and limited data. At some point the uncertainty limits the utility of these model predictions.

It is possible to use the methods presented here in a quantitative manor. In this study all quantitative aspects for each factor were reduced by nonparametric transformations to make factors directly comparable. For example the soluble phosphorus flow accumulation was an estimate of how much soluble phosphorus passed through the riparian buffer at any given location. If we were able to estimate the removal efficiency of the riparian buffer, we could determine the soluble phosphorus load reduction from the buffer. The same could be done for many of the factors. Other factors such as curvature may require additional research to quantify their effects. Curvature is ignored in watershed models, as are many other possible significant processes. It is possible to estimate the effect of each factor on the whole and estimate an improvement in water quality. Similar to watershed models, the uncertainty contained within this estimate would be unknown.

The method presented here was intended to be flexible and allow the inclusion of other riparian factors of interest. The optimal placement of buffers depends upon what is the intended function or functions of the buffers. Riparian buffers were considered in this study for sediment and nutrient removal, but they have many other benefits. Wildlife use riparian buffers as corridors to increase landscape connectivity. Riparian forest in low order streams provide shade which decreases water temperature and provide woody debris which enriches stream habitat and influences stream morphology. Indicators for many of these valuable riparian buffer services can be derived from readily available GIS data. Many of these benefits while important are difficult to quantify.

(3.3) Riparian Buffer Classification

The classification of riparian areas can be a useful tool. Most riparian inventories are based on landcover alone or on expensive field surveys. Factors developed as indicators of riparian effectiveness can be used with remote sensing algorithms to define sites with similar characteristics. With a few examples of highly effective riparian buffers within a basin, that signature can be defined and similar areas located within the basin or ecoregion for preservation. Similar areas with degraded landcover could be located and targeted for restoration. The entire

riparian area within a basin could be classified into categories, and each category could be rated for riparian buffer efficiency or function based on ground truth data. The result would be map of all riparian zones including characteristics of each class and level of functionality. Other data such as habitat assessments could be extrapolated from a few survey sites, to an entire basin. This method could be very useful for the inventory and assessment of riparian buffers within a basin.

(4) References

Alsleben, S., 2001, Point and polyline tools V1.2, http://arcscripts.esri.com/

Arnold, J. G., J. R. Willams, and D. R. Maidment, 1995, A continuous water and sediment routing model for large basin. J. Hydr. Engi., 121(2): 171-183.

Barling, R. D. and I. D. Moore, 1994, Role of buffer strips in managements of waterway pollution: a review. Environmental Management, 18: 543-558.

Christianson L. E., M. B. Armstrong, D. E. Storm, M. J. White, 2005, Evaluating Remote Sensing methods for targeting Erosion in Riparian Corridors, 2005 ASAE Annual International Meeting, City?, State? Paper Number: 052004

Fennessy, M. S. and J. K. Cronk, 1997, The effectiveness and restoration of riparian ecotones for the management of nonpoint source pollution, particular nitrate. Critical Reviews in Environmental Sciences and Technology, 27: 285-317.

Fields, S., 1992, Regulation and policies relating to the use of wetlands for nonpoint source control. Ecological Engineering, 1:135-142.

Furbish, D., 2001, Spatial autoregressive structure in meander evolution, Geological Society of America Bulletin, 103: 1576-1589

Hill, A. R., 1996, Nitrate removal in stream riparian zones. J. Environmental Quality, 25: 743-755.

Jin C. X., S. M. Dabney, and M. J. M. Romkens, 2002, Trapped mulch increases sediment removal by vegetative filter strips: a flume study. Transactions of the ASAE, 45(4): 929-939.

Jin C. X. and M. J. M. Romkems, 2001, Experimental studies of factors in determining sediment trapping in vegetative filter strips. Transactions of the ASAE, 44(2): 277-288.

Jin C. X., M. J. M. Romkens and F. Griffioen, 2000, Estimating Manning's roughness coefficient for shallow overland flow in non-submerged vegetative filter strips. Transactions of the ASAE, 43 (6): 1459-1466.

Lowrance, R., L. S. Altier, R. G. Williams, S. P. Inamdar, J. M. Sheridan, D. D. Bosch, R. K. Hubbard, and D. L. Thomas, 2000, REMM the riparian ecosystem management model, J. Water and Soil Conservation, Volume? (No.?)First Quarter, 27-34.

Lowrance, R., S. Dabney, and R. Schultz, 2002, Improving water and soil quality with conservation buffers, J. Water and Soil Conservation, 57(1): 36-43.

Marcelo C. and J. M. Conrad, 2003, The use of binary optimization and hydrologic models to form riparian buffers, J. Amer. Water Resour. Assoc., 39(5): 1167-1180.

Moore I. D. and J. P. Wilson, 1992, Length-slope factors for the Revised Universal Soil Loss Equation: simplified method of estimation, Journal of Soil and Water Conservation, 47(5), 423-428

Quinn, P.F. P. Beven, P. Chevallier, O. Planchon, 1991, The prediction of hillslope flow paths for distributed hydrological modeling using Digital Terrain Models, Hydrological Processes, (5): 59-79.

Renard, K.G., G.R. Foster, G.A. Weesies, and J.P. Porter. 1991, RUSLE: Revised Universal Erosion Equation. J. Soil and Water Conservation 46:30-33.

Schäuble, H., 2003, HydroTools 1.0 for ArcView 3.x, http://www.terracs.de/ArcView_3_x/HYDROTools/hydrotools.html

Singh A., R., Rudra, W., Yang, 2005, Adapting SWAT for Riparian Wetlands in an Ontario Watershed., 3rd International SWAT Conference Proceedings. (123-130).

Strahler, A., 1952, Dynamic basis of geomorphology. Geological Society of America Bulletin, 63, 923-938

Storm, D., M. White, and P. Busteed, 2005, Targeting high phosphorus loss areas in the Spavinaw Creek Basin FY 2003 319(h) C9-996100-11 Project 4 Spavinaw Creek Watershed Implementation Project EPA region 6

Tippett B. M., J. Sharp, E, Havens, and K, Hershner, 2001, GIS/GPS-based streamside assessment method for streamside restoration targeting Rapidan River watershed, Virginia , Coastal GeoTools '01. Proceedings of the 2nd Biennial Coastal GeoTools Conference. City? State? [np].

Tomer M. D., D. E. James, and T. M. Isenhart. 2003 Optimizing the placement of riparian practices in a watershed using terrain analysis. J. Soil and Water Conservation, 58(4): 198.

Wanhong Y. and A. Weersink, 2004, Cost-effective targeting of riparian buffers, Canadian J. Agricultural Economics. 52: 17–34

Wilkinson S., A. Jansen, R. Watts, A. Read, T. Miller, 2004 techniques for targeting protection and rehabilitation of riparian vegetation in the Middle and

Upper Murrumbidgee Catchment. CSIRO Land and Water Technical Report No. 37/04

Wischmeier, W.C., and D. D. Smith, 1978, Predicting rainfall erosion losses – a guide to conservation planning. Agriculture Handbook No. 537. US Dept Agric., Washington, DC.

Zhaoning, G., G. Huili; D. Wei, and Z. Wenji, 2005, The creation and analysis of riparian buffer zones based on RS and GIS - a case study on Beijing guanting watershed, Geoscience and Remote Sensing Symposium, IGARSS '05. Proceedings, 2005 IEEE International, 3: 1891-1895

1977, Procedure for computing rill and interrill erosion on project areas, SCS (NRCS) technical release 51.

1998, Stream Corridor Restoration: Principles, Processes, and Practices, Federal Interagency Stream Restoration Working Group (FISRWG)., http://www.nrcs.usda.gov/technical/stream_restoration/PDFFILES/ALL-SCRH-08-01.pdf, 5/2006